# Phenomenological and experimental searches for compressed stau-neutralino production at the LHC

**Manuel Alejandro Segura Delgado**[1]

Universidad de Los Andes[1] CO

September, 2019

# Outline


1. The Standard Model
   - Description and current issues
2. Physics beyond of the SM
   - Minimal Supersymmetric Standard Model
3. Large Hadron Collider - LHC
4. Compact Muon Solenoid - CMS
5. Research motivation
   - State of the Art
   - Phenomenological Study, third generation EWK-SUSY
   - QCD Multi-jets
   - Unblinded
   - Limit setting
6. Conclusions

# The Standard Model

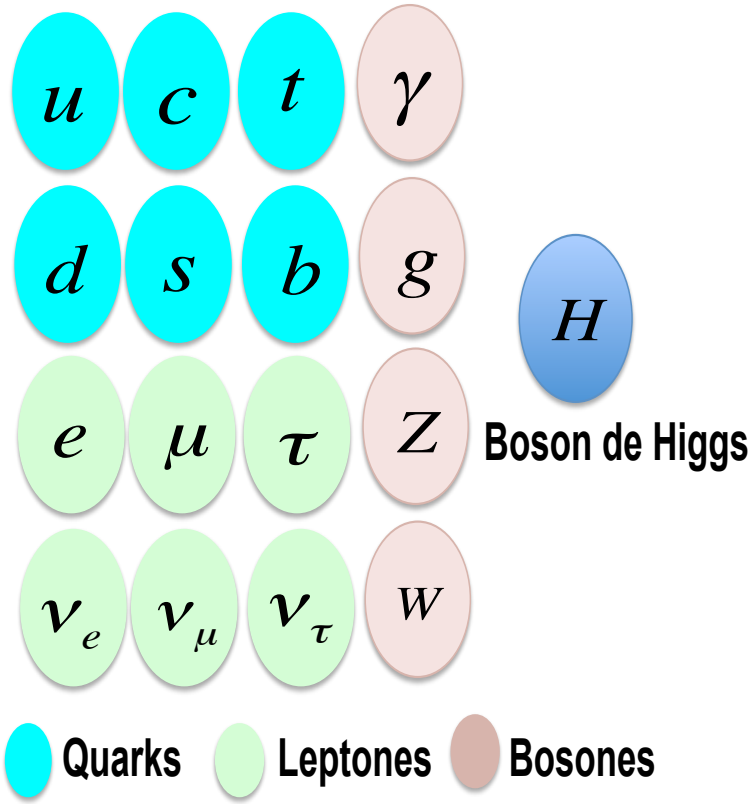


$$SU(3)_C \otimes SU(2)_L \otimes U(1)_Y$$

# The Standard Model

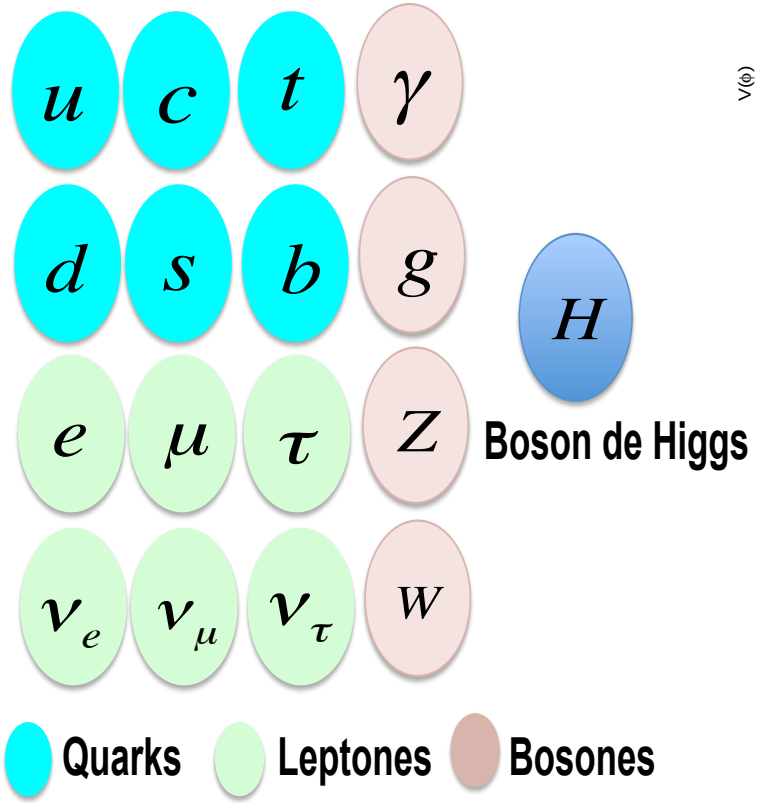


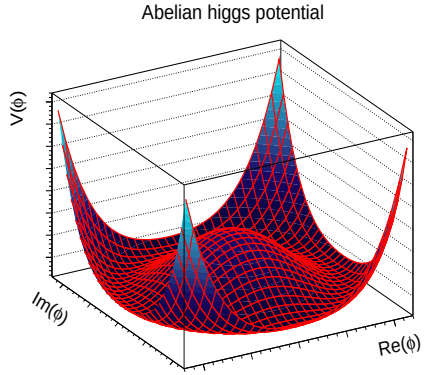


$$\mathcal{L}_H = (\mathcal{D}_\mu \phi)^\dagger (\mathcal{D}^\mu \phi) - \mu^2 (\phi^\dagger \phi) - \lambda (\phi^\dagger \phi)^2$$

$$SU(3)_C \otimes SU(2)_L \otimes U(1)_Y$$

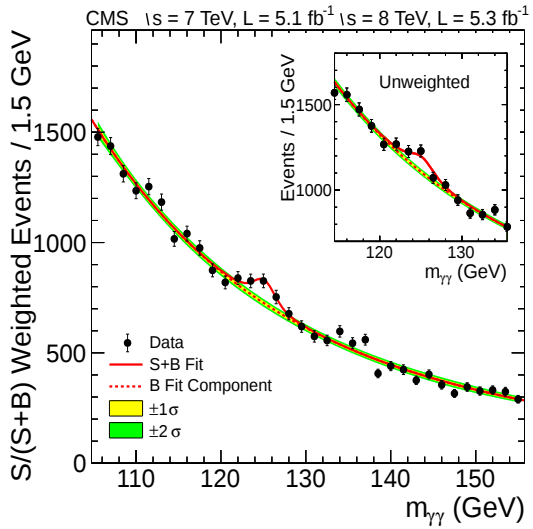


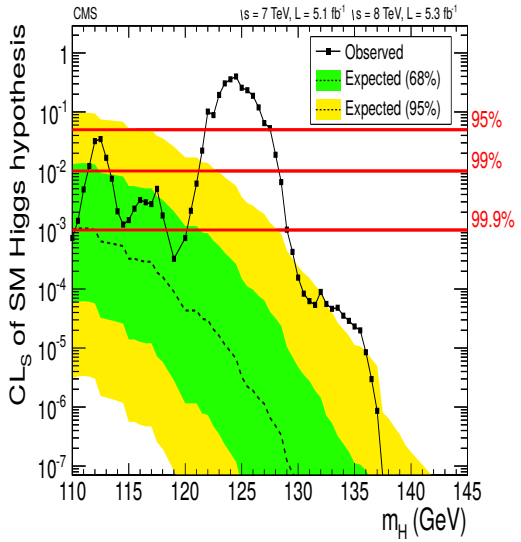

# Problems of the SM

- Hierarchy problem: Quantum corrections to the Higg's mass depend on the energy scale $\sim 10^{19}$ GeV.

$$\Delta m_H^2 = -\frac{|\lambda_f^2|}{8\pi^2}[\Lambda_{UV}^2 + ...]$$

- The Standard Model does not incorporate gravity effects.
- Why do neutrinos $\nu_e, \nu_\tau, \nu_\mu$ have mass?

# Problems of the SM

- Hierarchy problem: Quantum corrections to the Higg's mass depend on the energy scale $\sim 10^{19}$ GeV.

$$\Delta m_H^2 = -\frac{|\lambda_f^2|}{8\pi^2}[\Lambda_{UV}^2 + ...]$$

- The Standard Model does not incorporate gravity effects.
- Why do neutrinos $\nu_e, \nu_\tau, \nu_\mu$ have mass?

- The Dark matter and Dark energy:

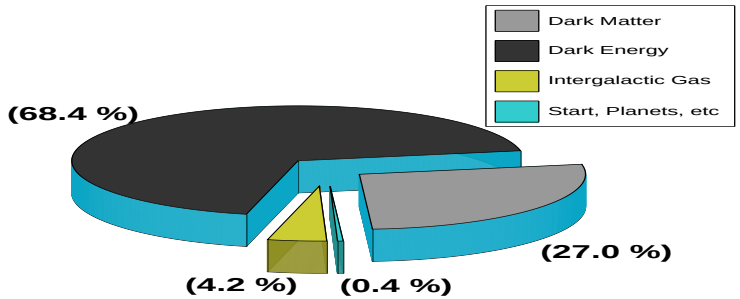


- Non-unification scheme for constant couplings in the Standard Model.

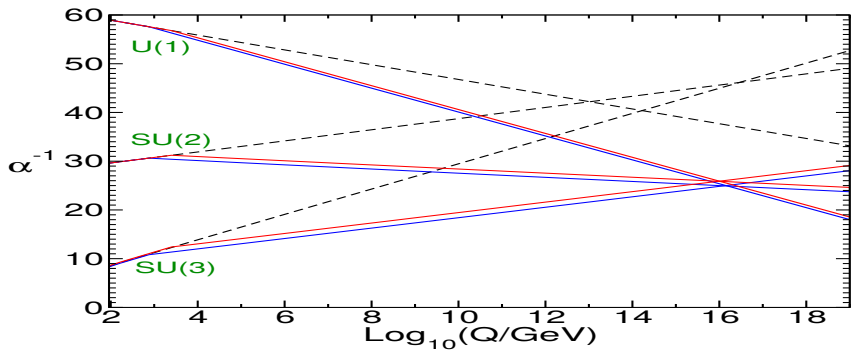

# Minimal Supersymmetric Standard Model (MSSM)

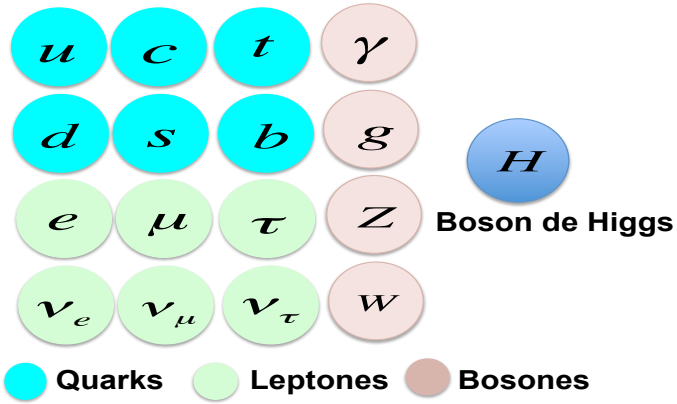


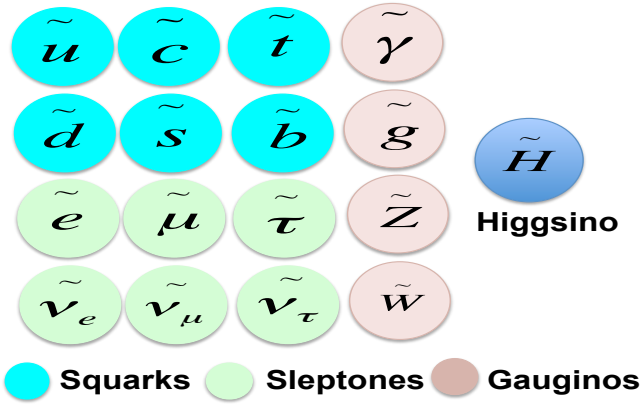

# Minimal Supersymmetric Standard Model (MSSM)

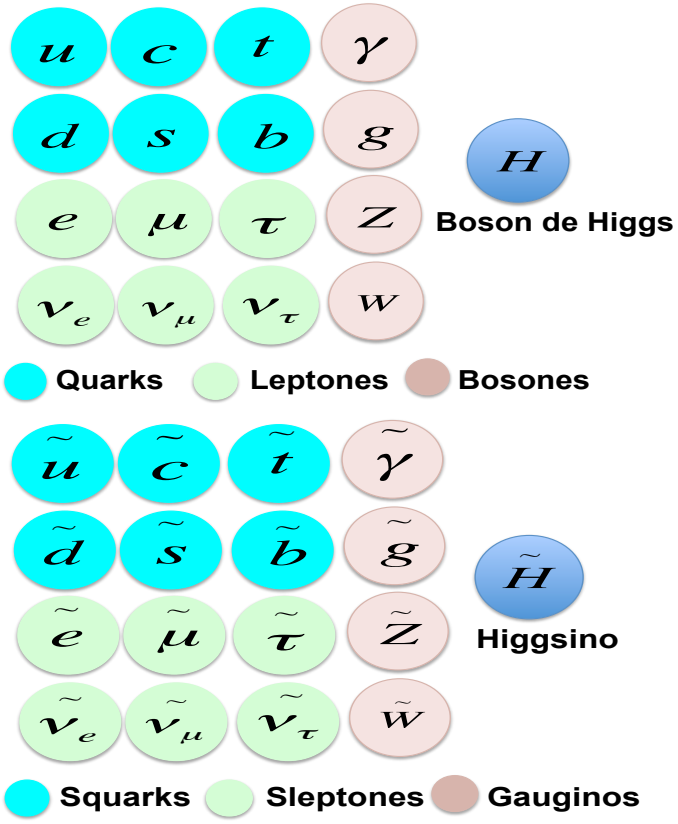


1. Higgs Sector

$$h_0, H^0, A^0, H^\pm$$

Associated Super-partners:

$$\tilde{H}_u^0, \tilde{H}_u^+, \tilde{H}_d^0, \tilde{H}_d^-$$

# Minimal Supersymmetric Standard Model (MSSM)

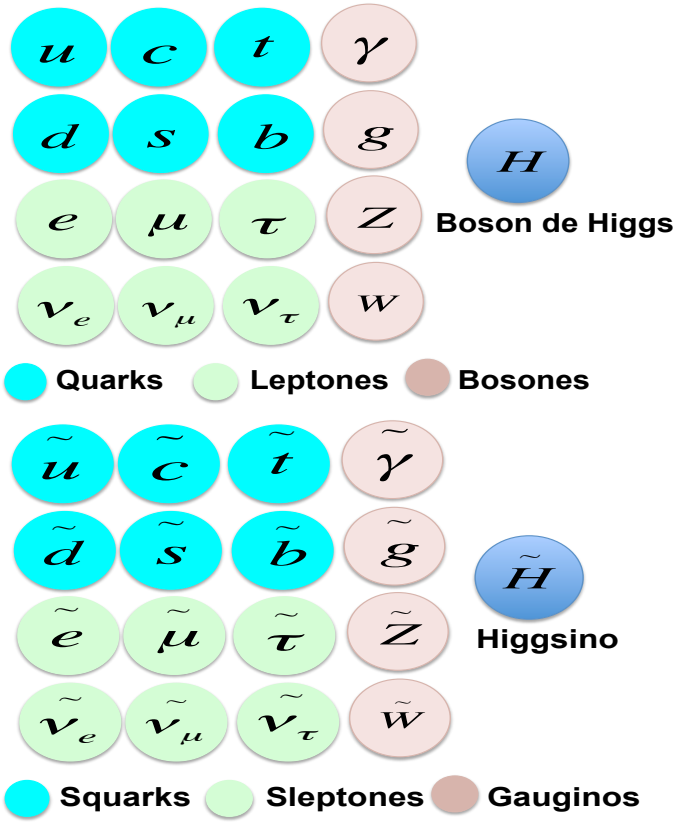


1. Higgs Sector
2. Electro-weak Sector

The mixing matrix of two higgsinos, wino $\tilde{W}^3$, and bino ($\tilde{B}$):

**Dirac-like fermions:**

$$M_C = \begin{pmatrix} M_2 & \sqrt{2} m_W \sin\beta \\ \sqrt{2} m_W \cos\beta & \mu \end{pmatrix}$$

$$U^* M_C V^\dagger = diag(m_{\tilde{\chi}_1^\pm}, m_{\tilde{\chi}_2^\pm}), \qquad m_{\tilde{\chi}_1^\pm} < m_{\tilde{\chi}_2^\pm}$$

**Majorana-like fermions:**

$$\begin{pmatrix} M_1 & 0 & -m_Z \cos\beta \sin\theta_W & m_Z \sin\beta \sin\theta_W \\ 0 & M_2 & m_Z \cos\beta \cos\theta_W & -m_Z \sin\beta \cos\theta_W \\ -m_Z \cos\beta \sin\theta_W & m_Z \cos\beta \cos\theta_W & 0 & -\mu \\ m_Z \sin\beta \sin\theta_W & -m_Z \sin\beta \cos\theta_W & \mu & 0 \end{pmatrix}$$

$$N^* M_N N^\dagger = diag(m_{\tilde{\chi}_1^0}, m_{\tilde{\chi}_2^0}, m_{\tilde{\chi}_3^0}, m_{\tilde{\chi}_4^0})$$

$$(m_{\tilde{\chi}_1^0} < m_{\tilde{\chi}_2^0} < m_{\tilde{\chi}_3^0} < m_{\tilde{\chi}_4^0})$$

# Minimal Supersymmetric Standard Model (MSSM)

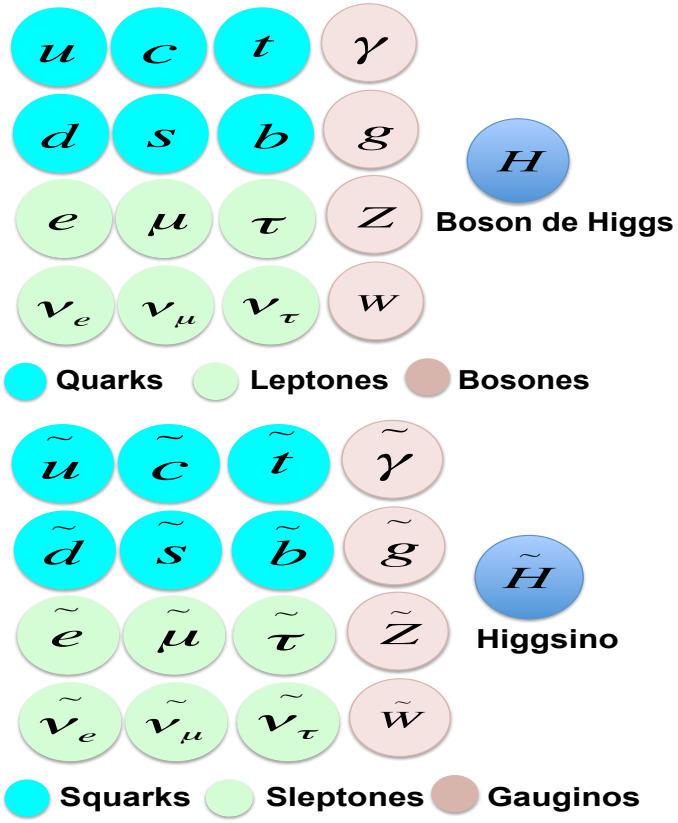


$$P_R = (-1)^{3(B-L)+2S}$$

- There are not composed states between SM and SUSY particles.
- SUSY particles are produced in pairs.
- From the previous item, the LSP must be **stable**. In MSSM, the LSP can be depending on the parametrization either neutralino ($\tilde{\chi}_1^0$) or gravitino ($\tilde{g}$). These hypothetical particles could explain DM.
- The super-partners must decay into an odd number of $\tilde{\chi}_1^0$ (it would explain the large amount of DM we observe in the universe).
- Hierarchy problem solved.

1. Higgs Sector
2. Electro-weak Sector
3. R-Parity

$$(\lambda - g^2)\Lambda^2\phi^\dagger\phi$$

# Experimental setup

1. The Large Hadron Collider

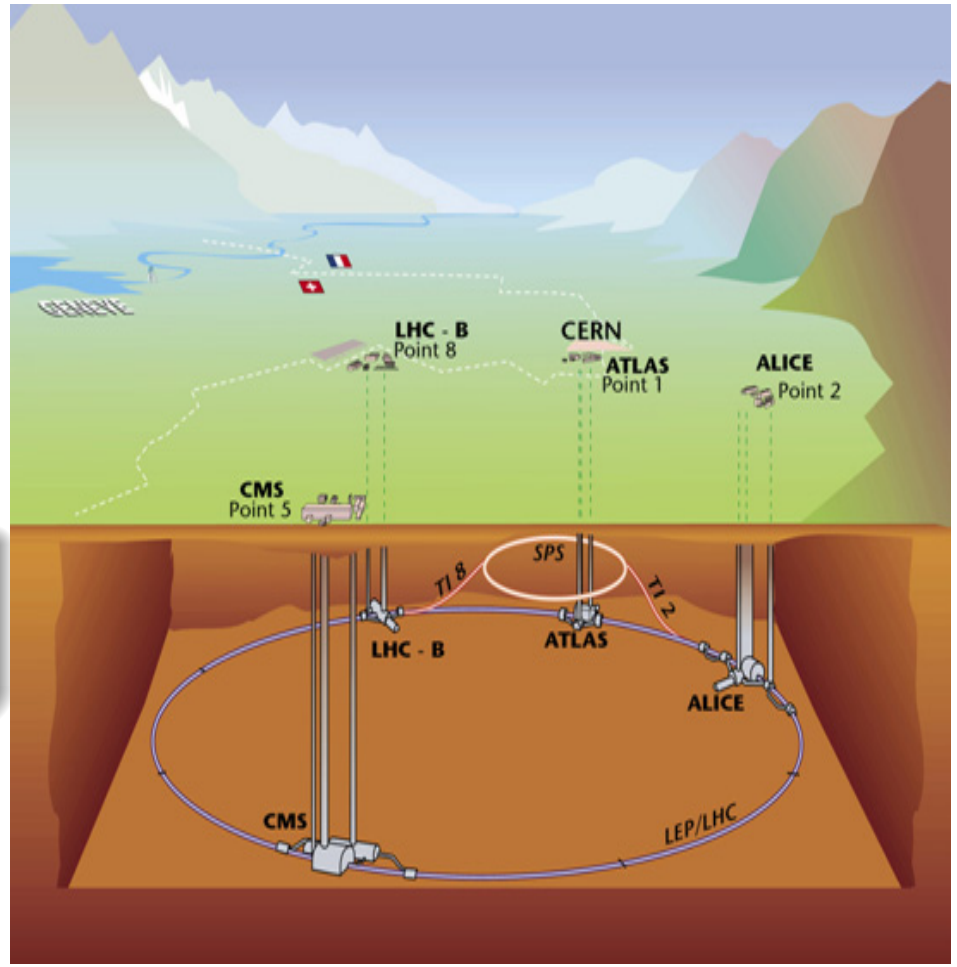


Sketch of the LHC inside of underground tunnel, the main experiments are: CMS, ATLAS, ALICE and LHCb

1. The Large Hadron Collider
2. Acceleration chain in the LHC

## Beam energy:

- LINAC2: $E = 50$ MeV
- Proton Synchrotron Booster (PSB): $E = 1.4$ GeV
- Proton Synchrotron (PS): $E = 25$ GeV
- Super Proton Synchrotron (SPS): $E = 450$ GeV
- LHC: $E = 6.5$ TeV

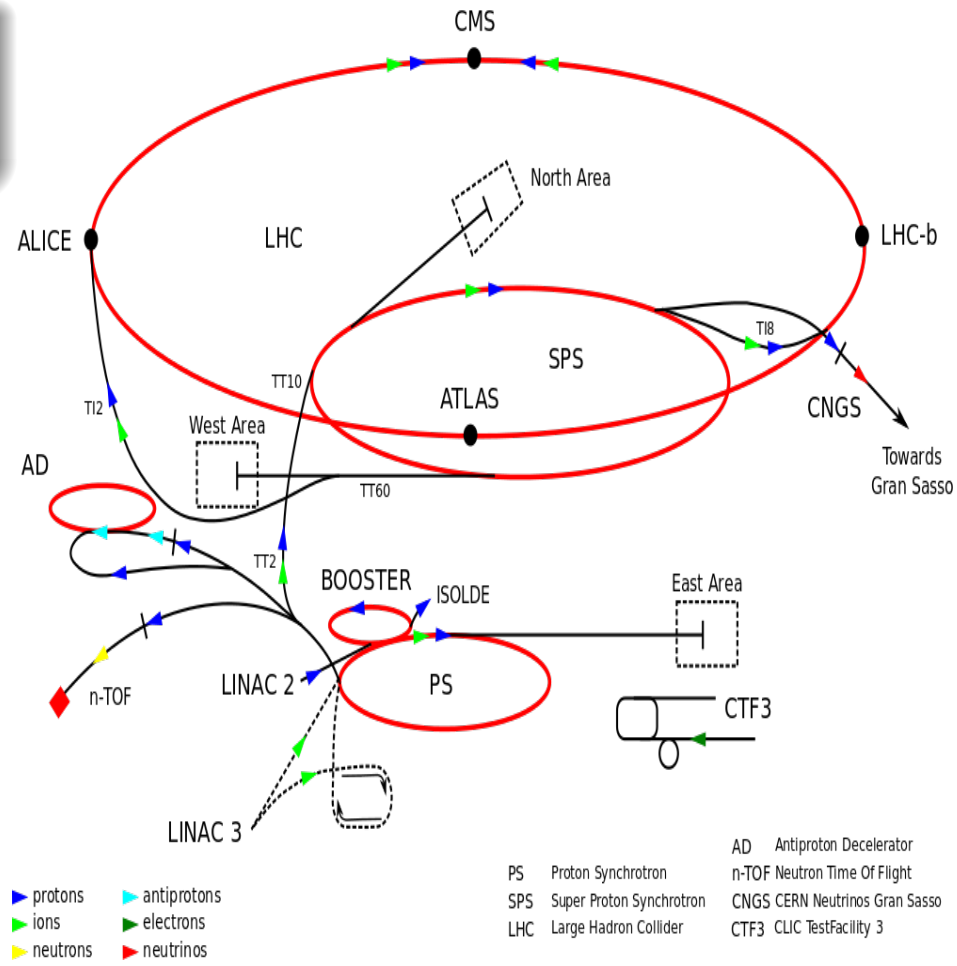

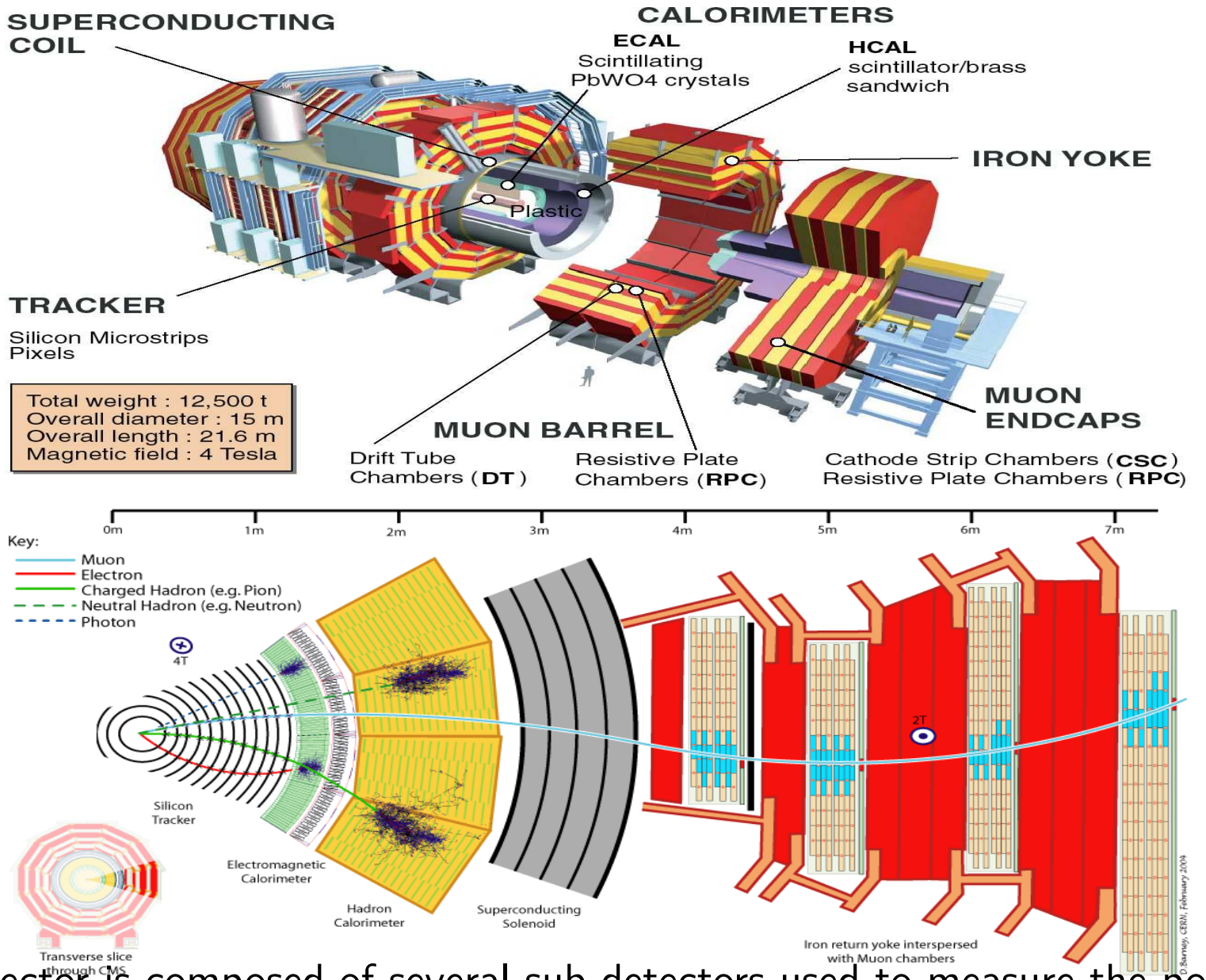


The detector is composed of several sub-detectors used to measure the position, momentum, and energy of the particles resulting from the collisions

# Research Motivation

# State of the Art

- Events with large missing transverse energy at CERN in 1987. $m(\tilde{q}) < 45$ GeV and $m(\tilde{g}) < 53$ GeV excluded.
- A search for squark and gluino production at the CERN pp collider in 1989. $m(\tilde{q}) < 74$ GeV and $m(\tilde{g}) < 79$ GeV excluded.
- Limits on the masses of supersymmetric particles from $\sqrt{s} = 1.8$ TeV $p\bar{p}$ collisions in 1990. $m(\tilde{g}) < 73$ GeV excluded.
- Experiments carried out by LEP between 1995-2000. $m(\tilde{\chi}_1^{\pm}) < 103.5$ GeV, $m(\tilde{\chi}_1^0) < 70$ GeV, $m(\tilde{\mu}) < 100$ GeV excluded.
- SUSY searches at the Tevatron in 2012. $160 < m(\tilde{b}) < 200$ GeV, $m(\tilde{\chi}_1^0) < 100$ GeV excluded.
- SUSY searches at LHC in 2012. $m(\tilde{t}) < 755$ GeV, $m(\tilde{\chi}_1^0) < 200$ GeV excluded.
- SUSY searches for electroweak production of charginos, neutralinos at LHC in 2014. $m(\tilde{\chi}_1^{\pm})$, $m(\tilde{\chi}_1^0)$ up to 720 GeV and sleptons up to 260 GeV excluded.
- SUSY searches for the **color sector** at CMS in 2018. $m(\tilde{t})$ up to 755 GeV for neutralino mass below 200 GeV excluded.
- SUSY searches for the **color sector** at ATLAS in 2018. $m(\tilde{g}) < 2000$ GeV excluded.
- SUSY searches for the **electroweak sector** at CMS in 2018. $\tilde{\chi}_1^{\pm}\tilde{\chi}_1^0$ Mass up to 710 GeV, $\tilde{\chi}^{\pm}\tilde{\chi}^{\mp}$ Mass up to 630 GeV.
- SUSY searches for the **electroweak sector** at ATLAS in 2018. $\tilde{\chi}_1^{\pm}\tilde{\chi}_1^0$ Mass up to 760 GeV, $\tilde{\chi}^{\pm}\tilde{\chi}^{\mp}$ Mass up to 630 GeV.

## Current Searches at LHC.

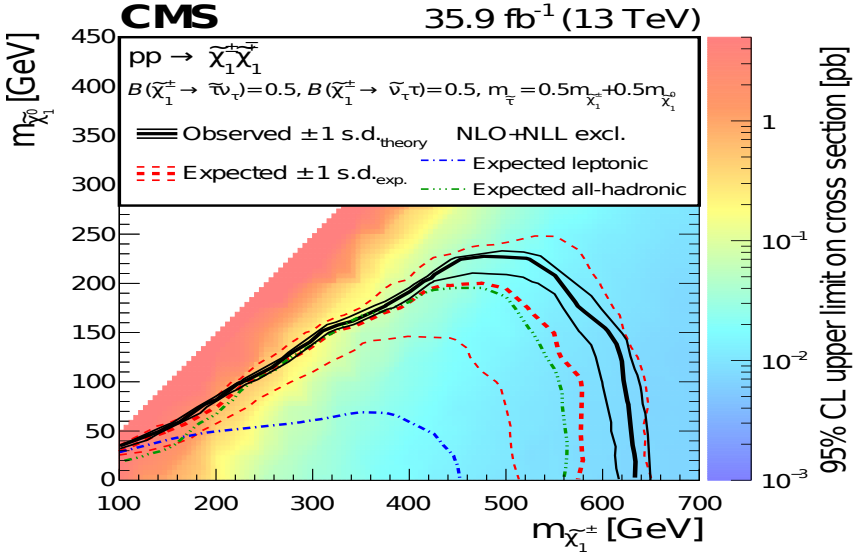


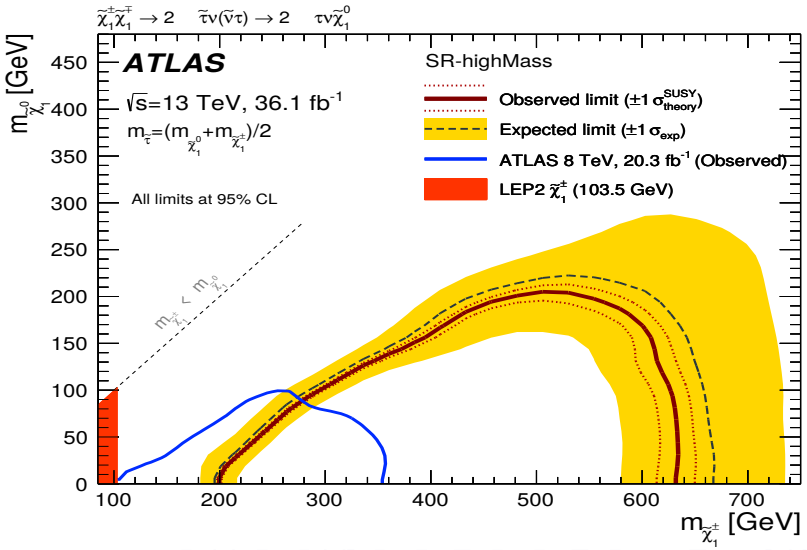

# Particle Physics, Cosmology, and Dark Matter

- To obtain a relic DM density consistent with the astronomically measured value, stau-neutralino *coannihilation* is one of the scenarios.
- The DM relic density is extremely sensitive to the mass difference between the stau ($\tilde{\tau}$) and the neutralino ($\tilde{\chi}_1^0$) $\rightarrow$ motivates a search for *compressed spectra* ($\Delta m < 50$ GeV).

$$\Omega_{\tilde{\chi}_1^0} h^2 \sim \int_0^{X_f} \frac{1}{< \sigma_{coann} \cdot \vec{v} >} dx$$

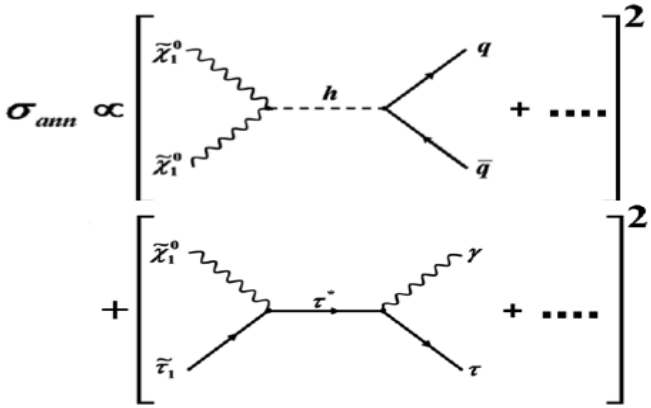


https://arxiv.org/pdf/1205.5842v1.pdf

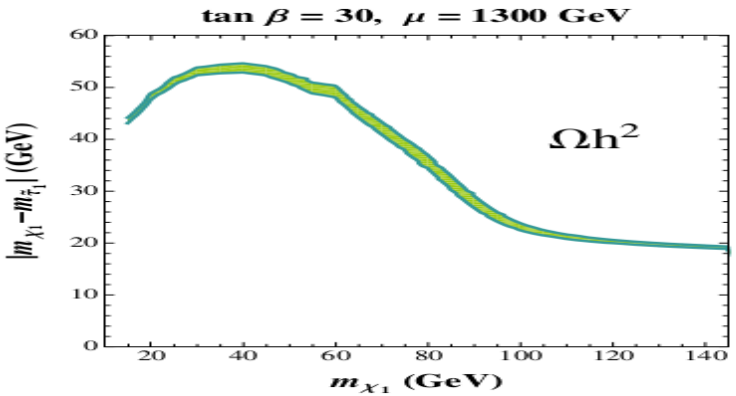


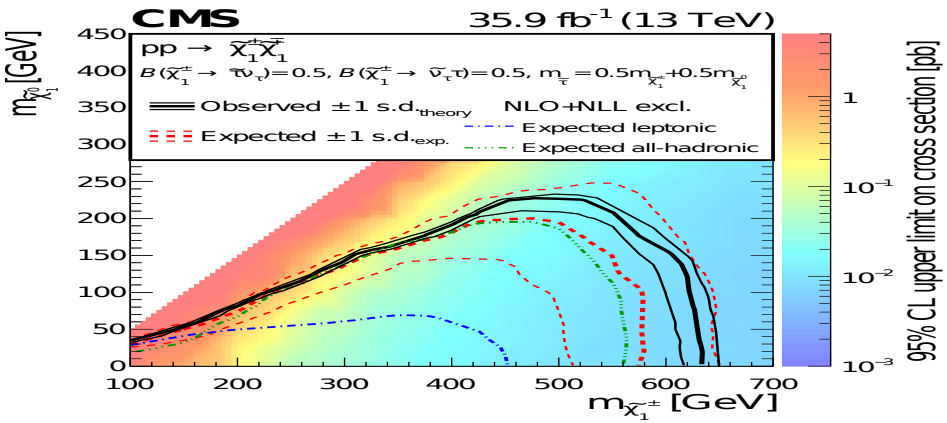

**Probing the Stau-Neutralino Coannihilation Region at the LHC with a soft tau lepton and an ISR jet**

Andrés Flórez[1], Luis Bravo[1], Alfredo Gurrola[2], Carlos Ávila[1], Manuel Segura[1], Paul Sheldon[2] and Will Johns[2]
[1] Physics Department, Universidad de los Andes, Bogotá, Colombia
[2] Department of Physics and Astronomy, Vanderbilt University, Nashville, TN, 37235, USA
(Dated: August 31, 2016)

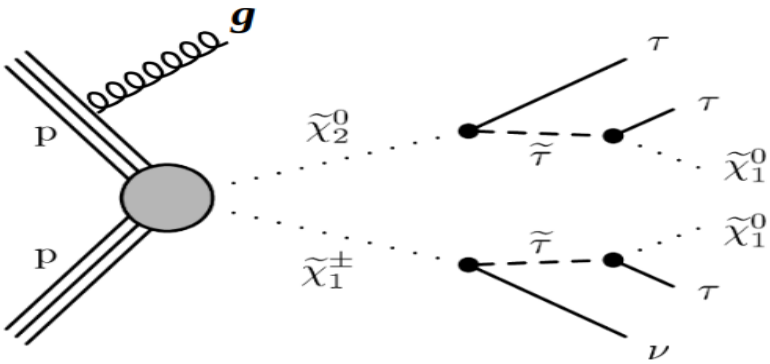


$$\begin{aligned} \vec{p}_T^{\,i} &= \vec{p}_T^{\,f} \\ 0 &= \vec{p}_T(\tau^+) + \vec{p}_T(\tau^-) \\ &+ \vec{p}_T^{\,1}(\tilde{\chi}_1^0) + \vec{p}_T^{\,2}(\tilde{\chi}_1^0) \end{aligned}$$

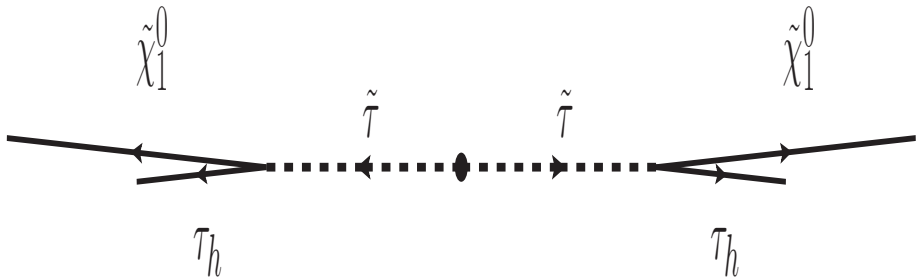


1. $\vec{p}_T^{\,1}(\tilde{\chi}_1^0) = -\vec{p}_T^{\,2}(\tilde{\chi}_1^0)$

- The $\tau$'s in compressed-mass spectra scenarios have low momentum with respect to $\tilde{\chi}_1^0$'s.

**Probing the Stau-Neutralino Coannihilation Region at the LHC with a soft tau lepton and an ISR jet**

Andrés Flórez[1], Luis Bravo[1], Alfredo Gurrola[2], Carlos Ávila[1], Manuel Segura[1], Paul Sheldon[2] and Will Johns[2]
[1] Physics Department, Universidad de los Andes, Bogotá, Colombia
[2] Department of Physics and Astronomy, Vanderbilt University, Nashville, TN, 37235, USA
(Dated: August 31, 2016)

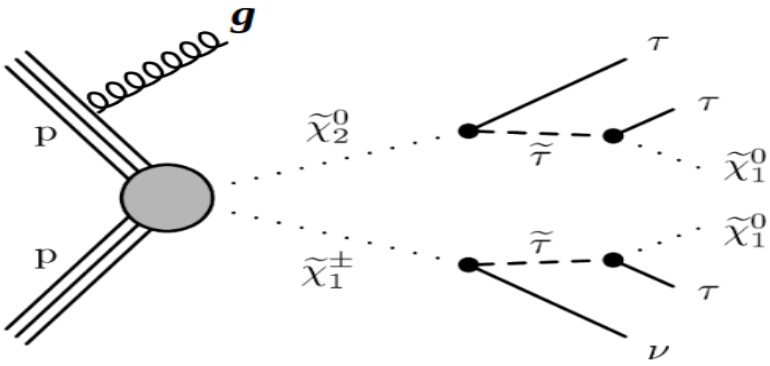


$$\begin{aligned} \vec{p}_T^{\,i} &= \vec{p}_T^{\,f} \\ 0 &= \vec{p}_T(\tau^+) + \vec{p}_T(\tau^-) \\ &+ \vec{p}_T^{\,1}(\tilde{\chi}_1^0) + \vec{p}_T^{\,2}(\tilde{\chi}_1^0) \end{aligned}$$

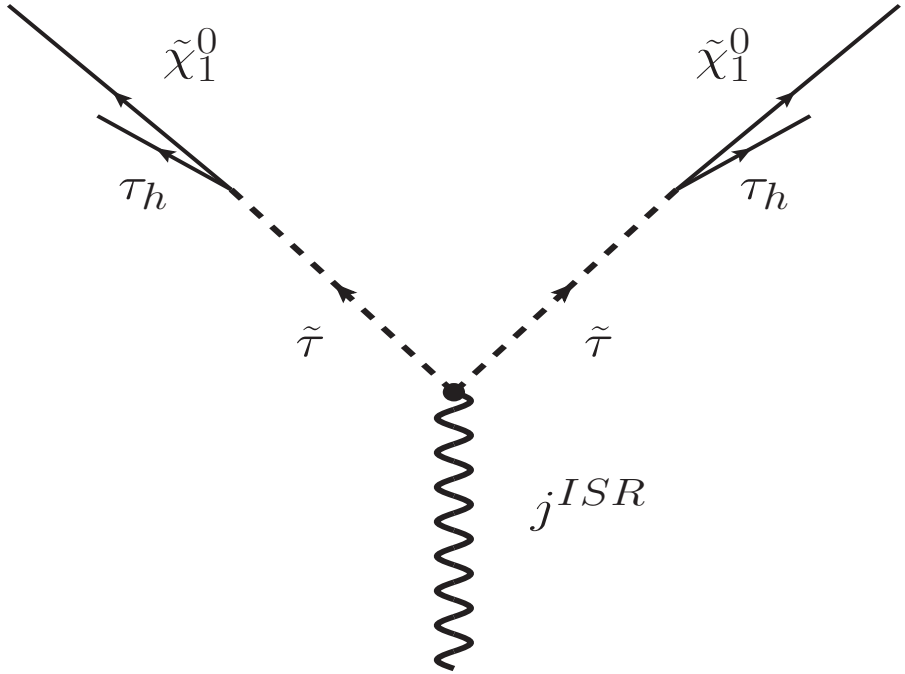


1. $\vec{p}_T^{\,1}(\tilde{\chi}_1^0) = -\vec{p}_T^{\,2}(\tilde{\chi}_1^0)$
2. $\vec{p}_T^{\,1}(\tilde{\chi}_1^0) = -\vec{p}_T^{\,2}(\tilde{\chi}_1^0) + \vec{p}_T^{\,j}(ISR)$

- The $\tau$'s in compressed-mass spectra scenarios have low momentum with respect to $\tilde{\chi}_1^0$'s.

**Probing the Stau-Neutralino Coannihilation Region at the LHC with a soft tau lepton and an ISR jet**

Andrés Flórez[1], Luis Bravo[1], Alfredo Gurrola[2], Carlos Ávila[1], Manuel Segura[1], Paul Sheldon[2] and Will Johns[2]
[1] Physics Department, Universidad de los Andes, Bogotá, Colombia
[2] Department of Physics and Astronomy, Vanderbilt University, Nashville, TN, 37235, USA
(Dated: August 31, 2016)

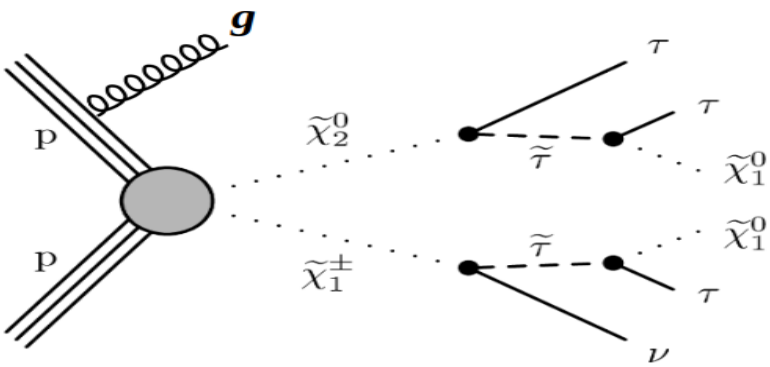


$$m_{\mathrm{T}}(\ell, p_{\mathrm{T}}^{miss}) = \sqrt{2 p_{\mathrm{T}}(\ell) p_{\mathrm{T}}^{miss} (1 - \cos \Delta\phi_{\ell, p_{\mathrm{T}}^{miss}})}$$

$$\begin{aligned} \vec{p}_T^{\,i} &= \vec{p}_T^{\,f} \\ 0 &= \vec{p}_T(\tau^+) + \vec{p}_T(\tau^-) \\ &+ \vec{p}_T^{\,1}(\tilde{\chi}_1^0) + \vec{p}_T^{\,2}(\tilde{\chi}_1^0) \end{aligned}$$

1. $\vec{p}_T^{\,1}(\tilde{\chi}_1^0) = -\vec{p}_T^{\,2}(\tilde{\chi}_1^0)$
2. $\vec{p}_T^{\,1}(\tilde{\chi}_1^0) = -\vec{p}_T^{\,2}(\tilde{\chi}_1^0) + \vec{p}_T^{\,j}(ISR)$

- The $\tau$'s in compressed-mass spectra scenarios have low momentum with respect to $\tilde{\chi}_1^0$'s.

Event Selection Criteria for SR.

| Criteria | Value |
|---|---|
| $N(j^{lead})$ | $\geq 1$ |
| $p_T(j^{lead})$(Boost) | 100 GeV |
| $\lvert\eta(j^{lead})\rvert$ | $\leq 2.5$ |
| $N(\tau_h)$ | 1 |
| $N(e^-/\mu^-)$ | 0 |
| $N(b-jet)$ | 0 |
| $p_T(\tau_h)$ | $> 15$ & $< 35$ GeV |
| $\lvert\eta(\tau_h)\rvert$ | $\leq 2.3$ |
| $\Delta R(\tau_h, j)$ | $> 0.3$ |
| $p_T^{miss}$ | $> 230$ |

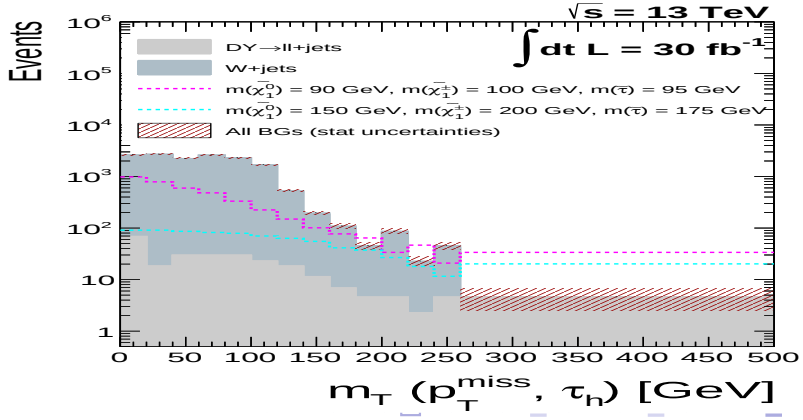

# Experimental study

# Background estimation

$$N_{\mathrm{SR}} = \sigma \cdot L_{\mathrm{int}} \cdot \epsilon_{\mathrm{b-jet}} \cdot \epsilon_{\tau_h} \cdot \epsilon_{p_{\mathrm{T}}^{miss}} \cdot \epsilon_{\mathrm{ISR}}$$

# QCD Multi-jets contribution

- We use the classic ABCD method to estimate the QCD Multi-jets contribution in the SR.
- This method allows to obtain the $m_{\mathrm{T}}$ shape and a correct normalization factor.
- Loose-Tight means that a $\tau_h$ candidate passes Loose but fails Tight isolation requirement.
- Since the strong mismodelling of QCD events in MC, the semi-data driven approach leads to different scale factor for the normalization.

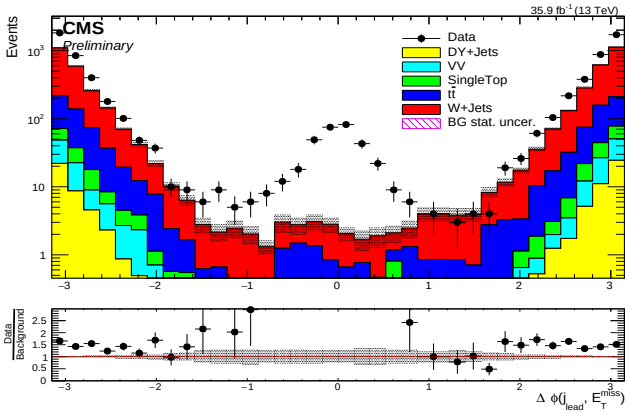


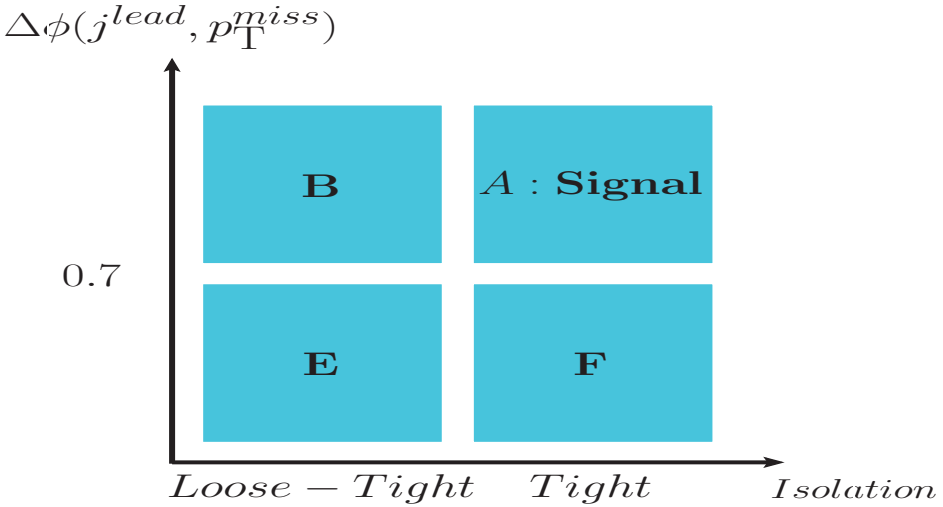

# QCD Multi-jets contribution

- We use the classic ABCD method to estimate the QCD Multi-jets contribution in the SR.
- This method allows to obtain the $m_{\mathrm{T}}$ shape and a correct normalization factor.
- Loose-Tight means that a $\tau_h$ candidate passes Loose but fails Tight isolation requirement.
- Since the strong mismodelling of QCD events in MC, the semi-data driven approach leads to different scale factor for the normalization.

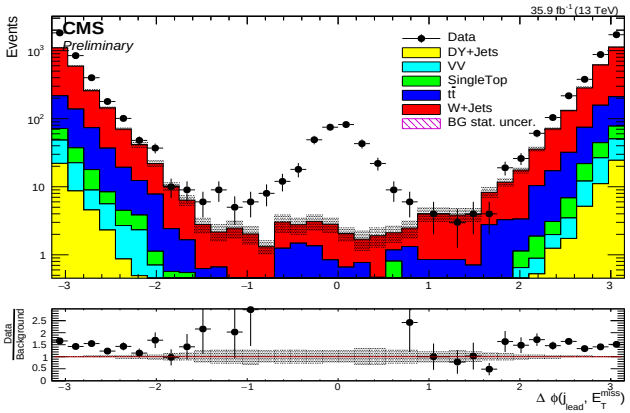


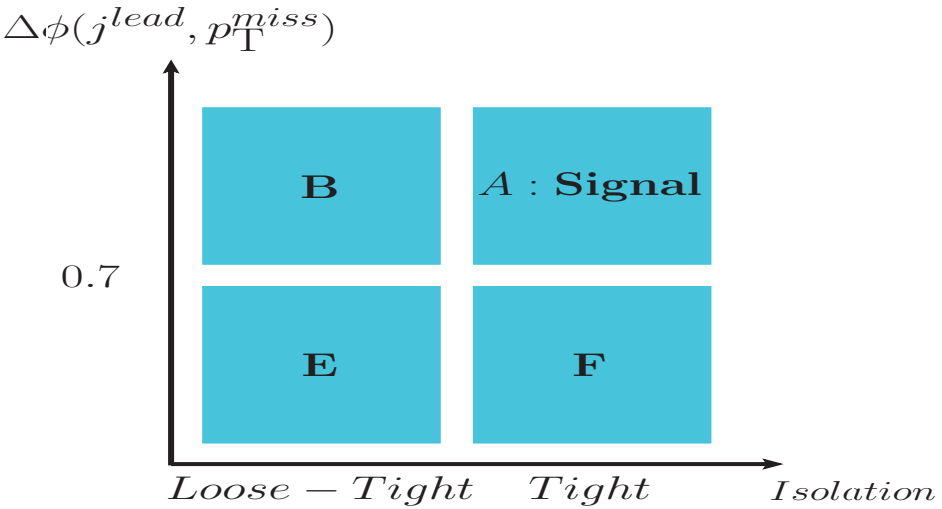


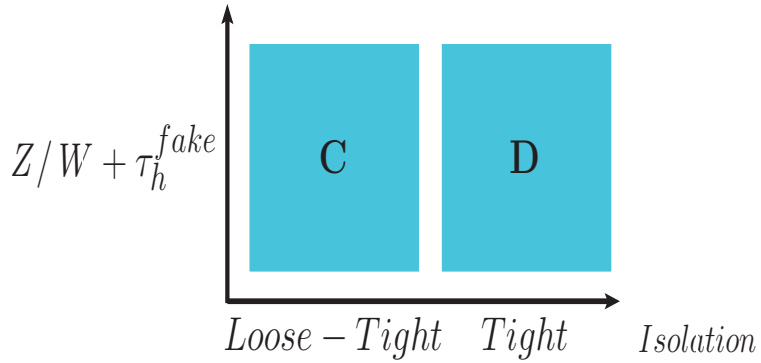


1. Fully data-driven approach is used.

# QCD Multi-jets contribution: closure test

- To validate the extraction of the shape from the non-isolated events and the $p_{\mathrm{T}}(\tau_h)$ dependent $R^{Tight}_{Loose}$ ratios, CRE and CRF are used.

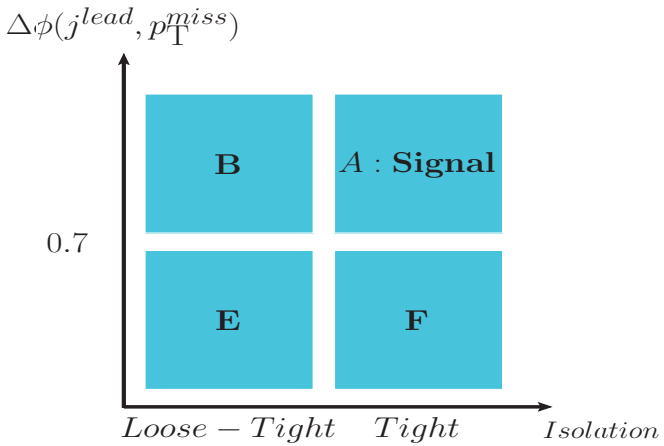

# QCD Multi-jets contribution: closure test

- To validate the extraction of the shape from the non-isolated events and the $p_{\mathrm{T}}(\tau_h)$ dependent $R^{Tight}_{Loose}$ ratios, CRE and CRF are used.

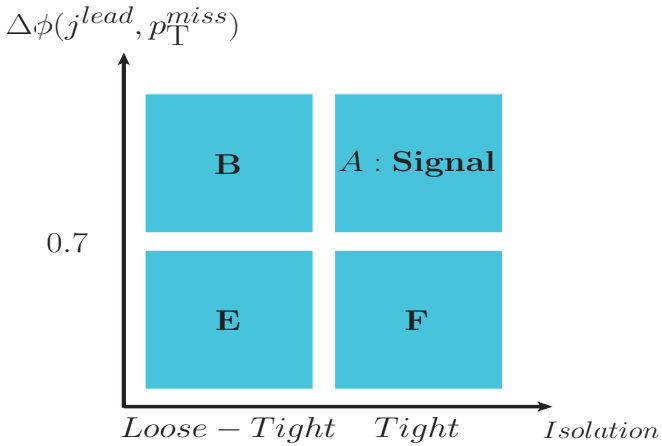


1. 2D histogram represents the predicted yield of QCD-multijes events in CRE (left) and CRF (right), as a function of $m_{\mathrm{T}}(\tau_h, p_{\mathrm{T}}^{miss})$ and $p_{\mathrm{T}}(\tau_h)$.

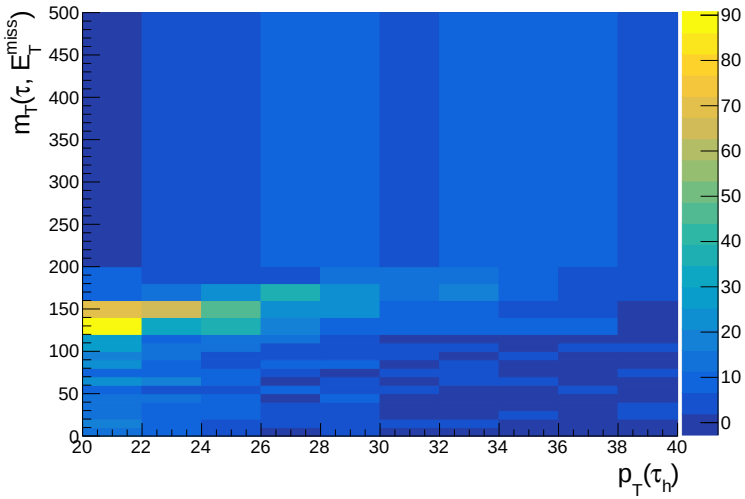


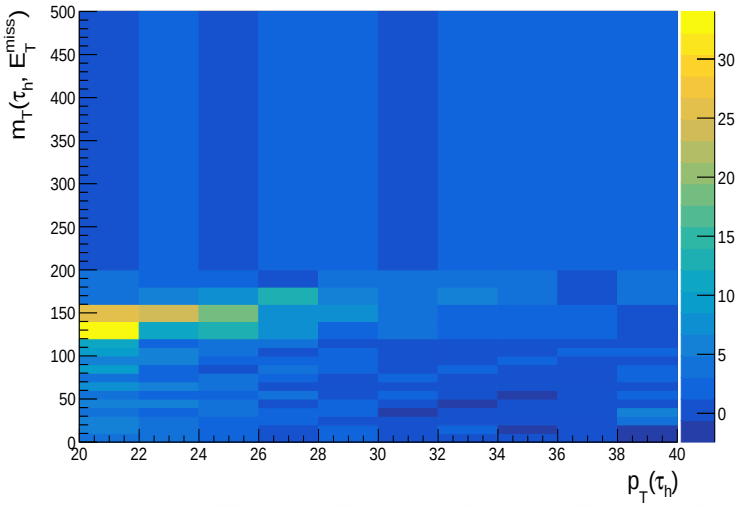

# QCD Multi-jets contribution: closure test

- To validate the extraction of the shape from the non-isolated events and the $p_{\mathrm{T}}(\tau_h)$ dependent $R^{Tight}_{Loose}$ ratios, CRE and CRF are used.

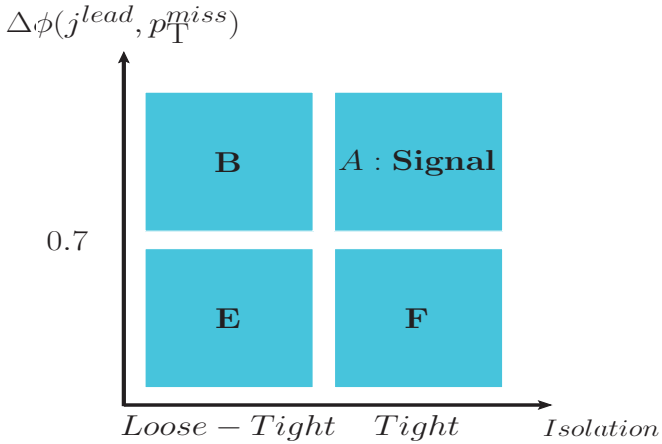


1. 2D histogram represents the predicted yield of QCD-multijes events in CRE (left) and CRF (right), as a function of $m_{\mathrm{T}}(\tau_h, p_{\mathrm{T}}^{miss})$ and $p_{\mathrm{T}}(\tau_h)$.
2. Final yield of QCD Multi-jets events in CRF.

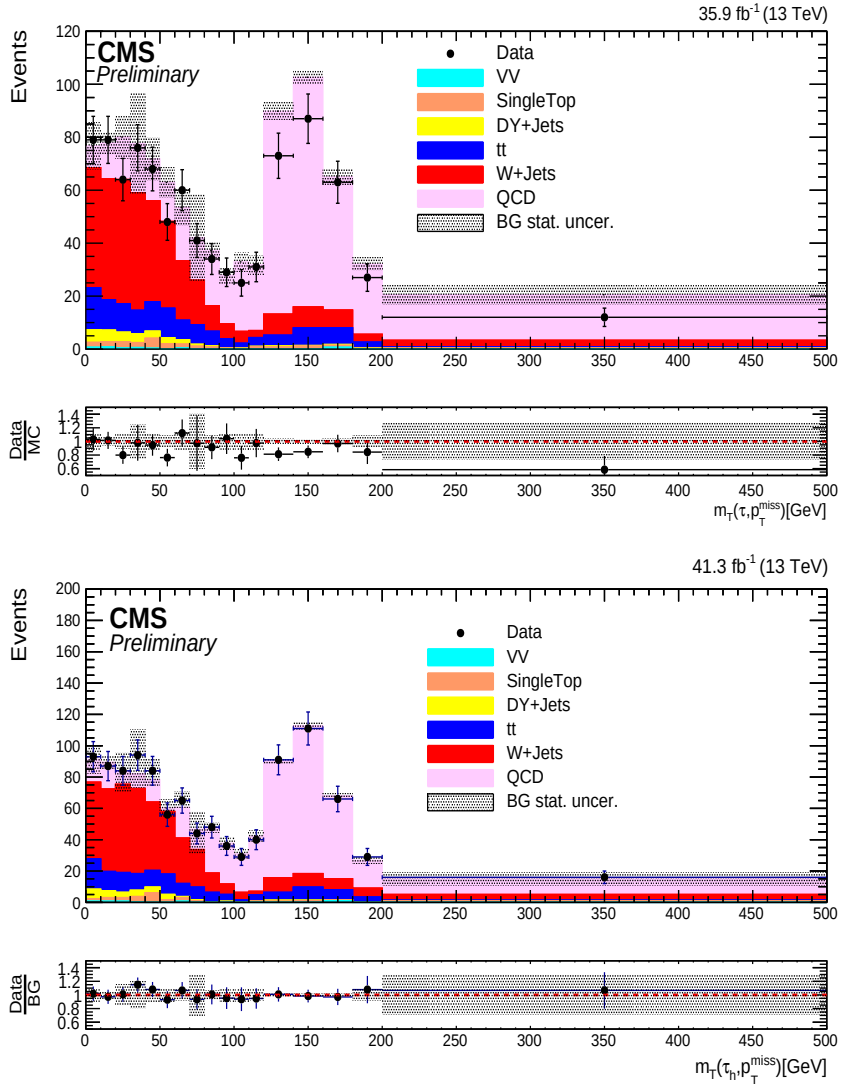


2016 (top) and 2017 (bottom)

# Unblinded plots

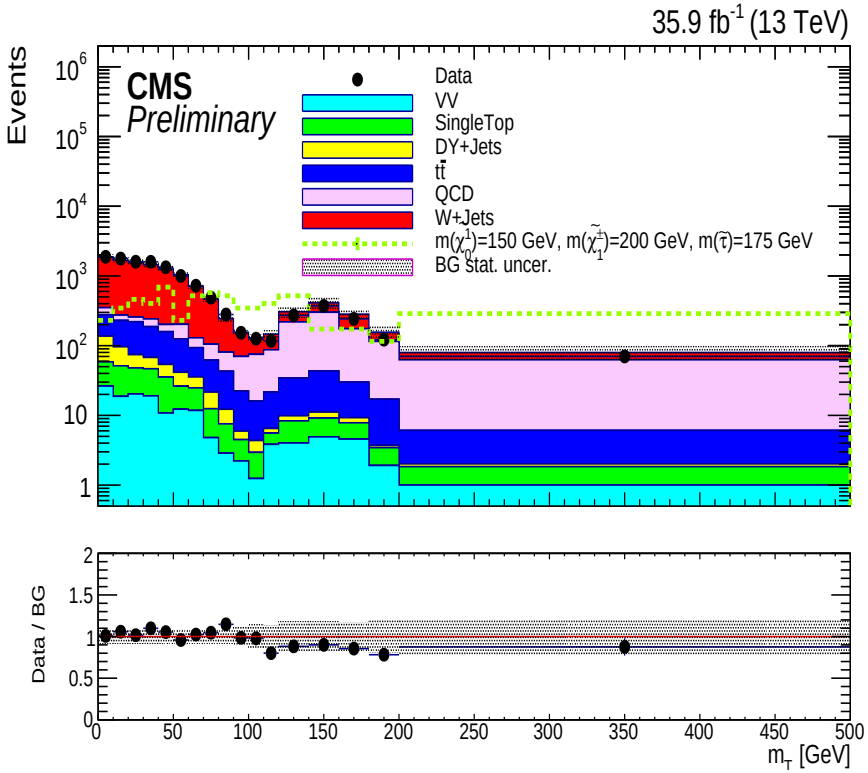


$m_{\mathrm{T}}(\tau_h, p_{\mathrm{T}}^{miss})$ unblinded for 2016 data and MC

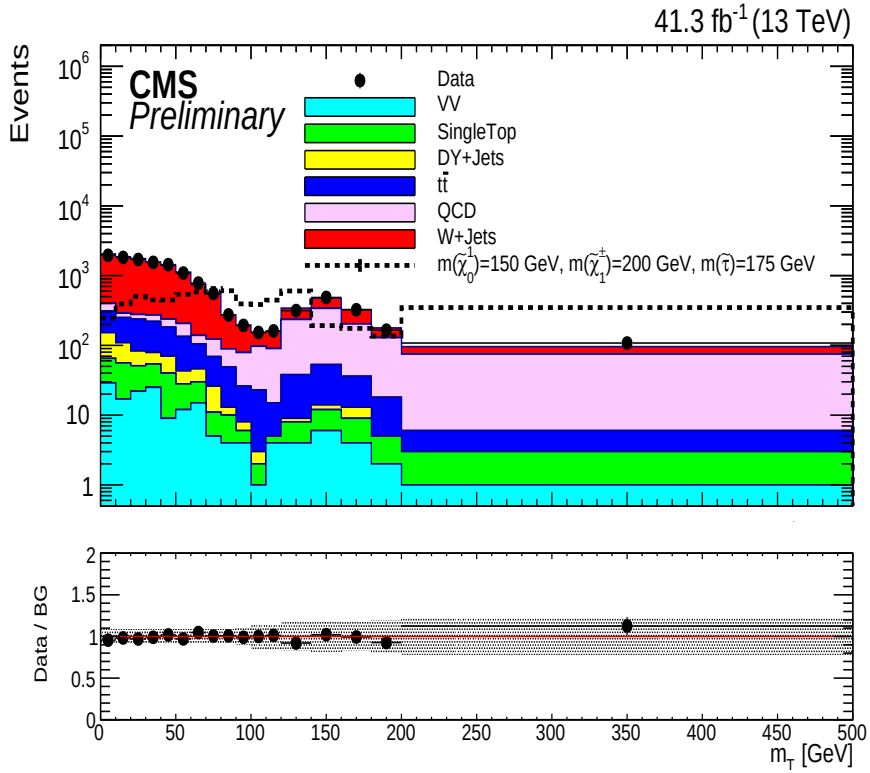


$m_{\mathrm{T}}(\tau_h, p_{\mathrm{T}}^{miss})$ unblinded for 2017 data and MC

# Unblinded plots

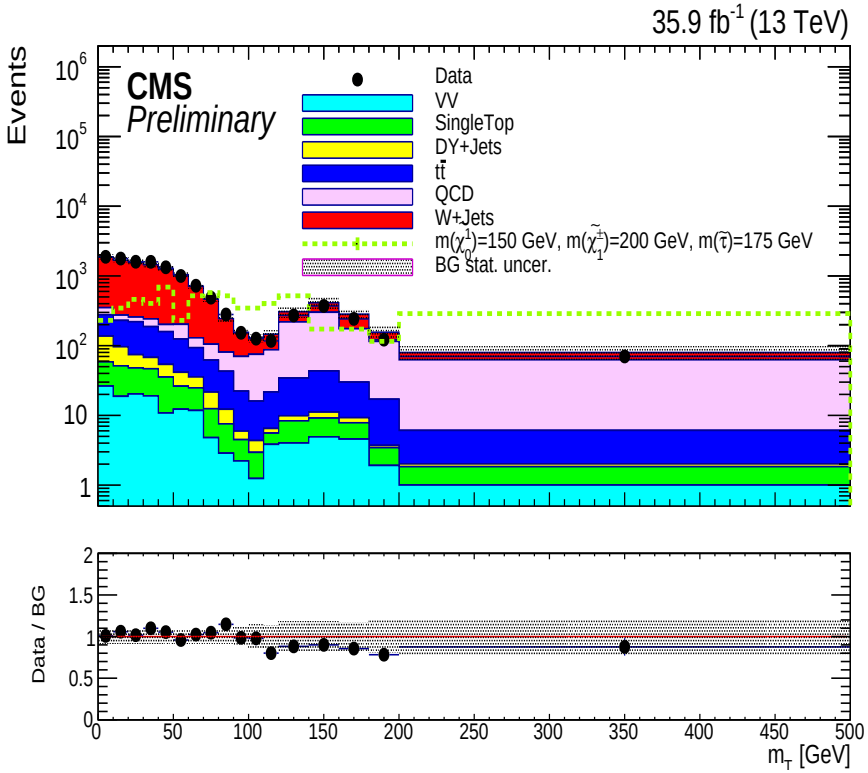


$m_{\mathrm{T}}(\tau_h, p_{\mathrm{T}}^{miss})$ unblinded for 2016 data and MC

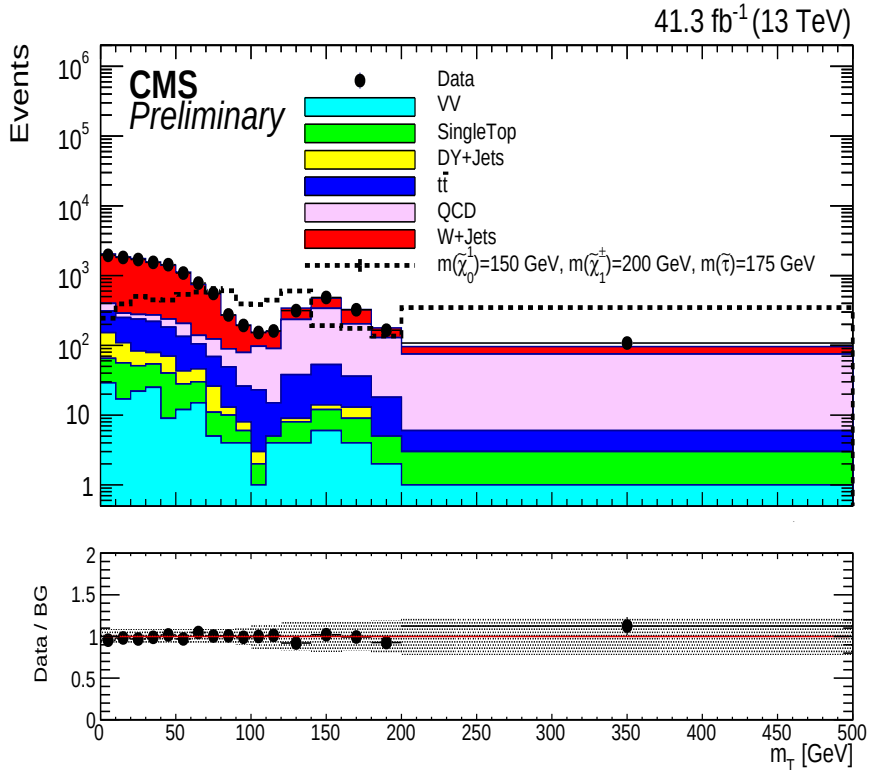


$m_{\mathrm{T}}(\tau_h, p_{\mathrm{T}}^{miss})$ unblinded for 2017 data and MC

There is no evidence of new physics in this research!

# Expected and observed limits

- Signal are inclusive $N(j) \leq 2$ in MadGraph
- $\tilde{\chi}_2^0$ and $\tilde{\chi}_1^\pm$ are 100% Wino
- $\tilde{\chi}_1^0$ is 100% Bino
- $m(\tilde{\chi}_1^\pm) - m(\tilde{\chi}_1^0) = 50$ GeV
- $m(\tilde{\tau}) = 0.5m(\tilde{\chi}_1^\pm) + 0.5m(\tilde{\chi}_1^0)$
- Inclusive $\tilde{\tau}$ production:
  - $\tilde{\chi}_1^\pm\tilde{\chi}_2^0$+jets ($\sim$ 64.4% of total x-sec)
  - $\tilde{\chi}_1^\pm\tilde{\chi}_1^\pm$+jets ($\sim$ 33% of total x-sec)
  - $\tilde{\chi}_1^\pm\tilde{\chi}_1^\mp$+jets, $\tilde{\chi}_2^0\tilde{\chi}_2^0$+jets, $\tilde{\chi}_1^\pm\tilde{\chi}_1^0$+jets, $\tilde{\chi}_2^0\tilde{\chi}_1^0$+jets
  - $\tilde{\tau}\tilde{\tau}$+jets ($\sim$ 2% of the total x-sec)

# Expected and observed limits

- Signal are inclusive $N(j) \leq 2$ in MadGraph
- $\tilde{\chi}_2^0$ and $\tilde{\chi}_1^\pm$ are 100% Wino
- $\tilde{\chi}_1^0$ is 100% Bino
- $m(\tilde{\chi}_1^\pm) - m(\tilde{\chi}_1^0) = 50$ GeV
- $m(\tilde{\tau}) = 0.5m(\tilde{\chi}_1^\pm) + 0.5m(\tilde{\chi}_1^0)$
- Inclusive $\tilde{\tau}$ production:
  - $\tilde{\chi}_1^\pm \tilde{\chi}_2^0$+jets ($\sim$ 64.4% of total x-sec)
  - $\tilde{\chi}_1^\pm \tilde{\chi}_1^\pm$+jets ($\sim$ 33% of total x-sec)
  - $\tilde{\chi}_1^\pm \tilde{\chi}_1^\mp$+jets, $\tilde{\chi}_2^0 \tilde{\chi}_2^0$+jets, $\tilde{\chi}_1^\pm \tilde{\chi}_1^0$+jets, $\tilde{\chi}_2^0 \tilde{\chi}_1^0$+jets
  - $\tilde{\tau}\tilde{\tau}$+jets ($\sim$ 2% of the total x-sec)

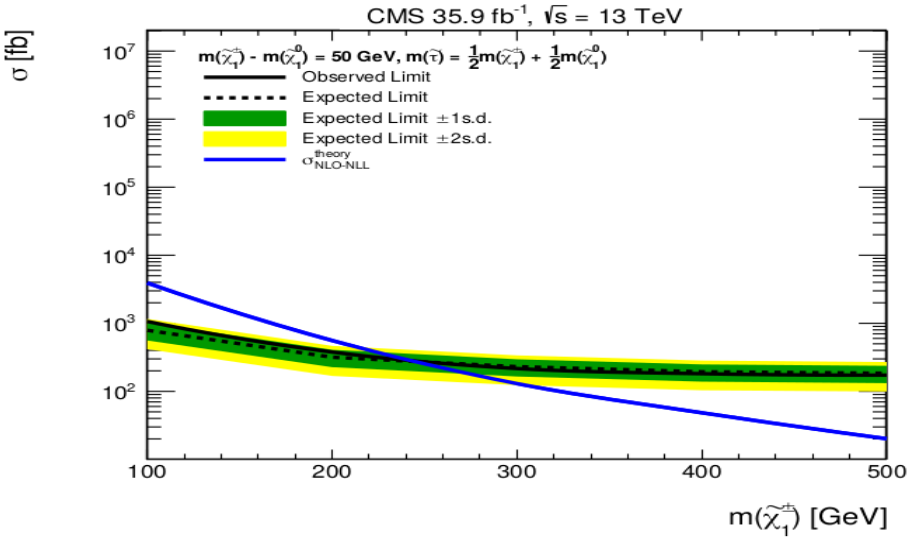


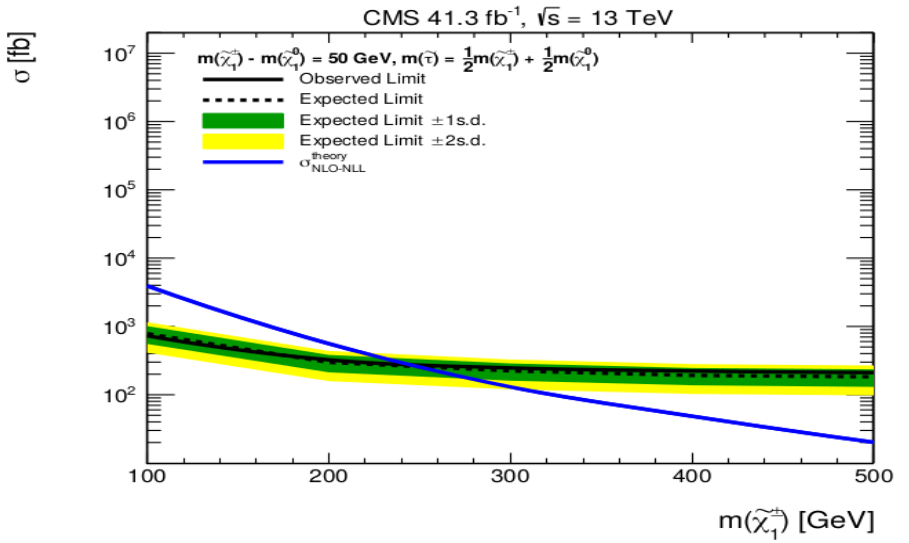


1. Expected and observed upper limit at the 95% CL on signal cross-section as a function of $m(\tilde{\chi}_2^0) = m(\tilde{\chi}_1^\pm)$ 2016 (top) & 2017 (bottom) data.

# Combined limits

1. Expected and observed upper limit at the 95% CL on signal cross-section as a function of $m(\tilde{\chi}_2^0) = m(\tilde{\chi}_1^\pm)$ for combined 2016 & 2017 datasets.

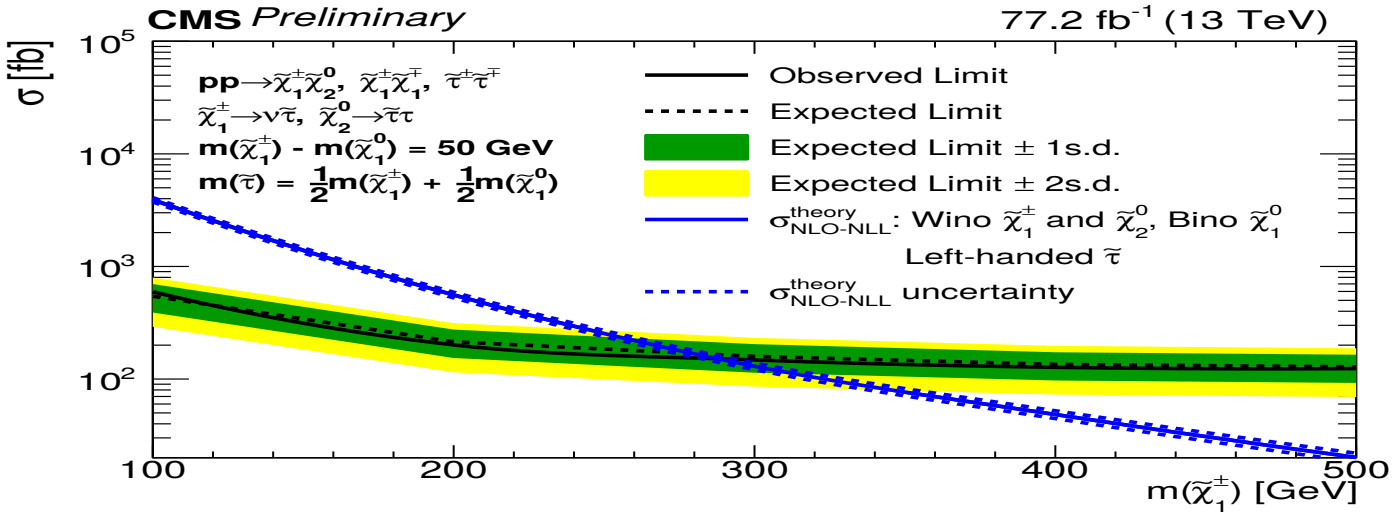


We exclude $\tilde{\chi}_2^0/\tilde{\chi}_1^\pm$ with masses below 290 GeV for $m(\tilde{\chi}_1^\pm) - m(\tilde{\chi}_1^0) = 50$ GeV exceeding the sensitivity from other searches in theses compressed $\tilde{\tau} - \tilde{\chi}_1^0$ regions. Previous limits from LEP excluded masses below $\sim 100$ GeV.

# Combined limits

1. Expected and observed upper limit at the 95% CL on signal cross-section as a function of $m(\tilde{\chi}_2^0) = m(\tilde{\chi}_1^{\pm})$ for combined 2016 & 2017 datasets.
2. Expected and observed upper limit at the 95% CL on signal cross-section as a function of $m(\tilde{\tau})$ for combined 2016 & 2017 datasets.

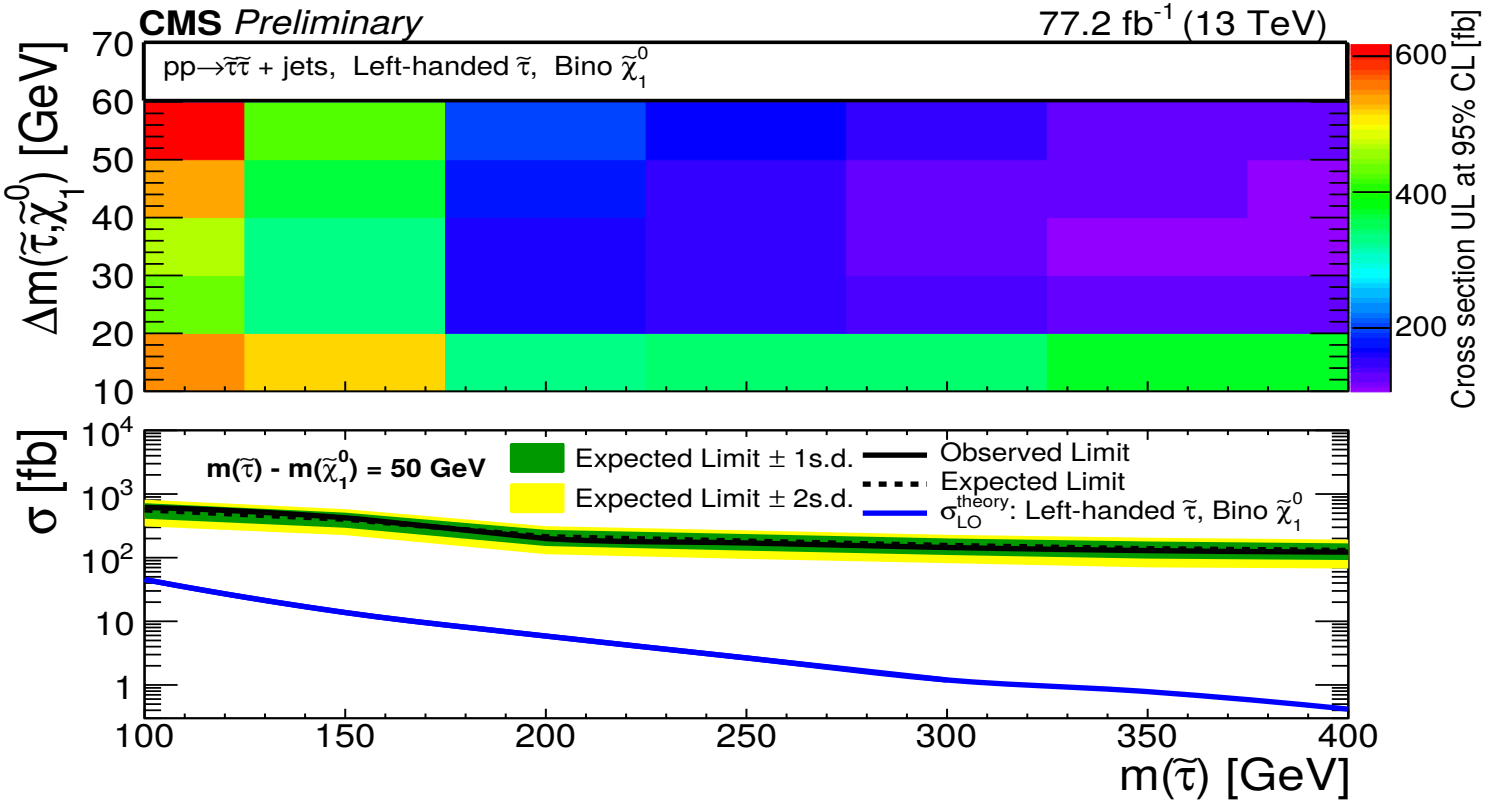

# Summary and Conclusions

- CMS initiated SUSY search in $\tilde{\tau} - \tilde{\chi}_1^0$ coanaihilation scenarios using ISR jet.
- Studies on $\mathrm{Z}(\rightarrow \mu^+\mu^-) + \mathrm{ISR}$ resulted in the boson boost weights for 2016/2017 data.
  - The efficiency $\epsilon_{\mathrm{ISR}}$ is well-understood.
  - After further study into jet resolution, $\epsilon_{\mathrm{MET}}$ is also well-understood.
- Those boson weights (and modeling of the $p_T^{miss}$) were validated on a region of $\mathrm{W}(\rightarrow \mu\nu) + \mathrm{ISR}$ for 2016/2017 data.
- $\mathrm{Z}(\rightarrow \tau^+\tau^-) + \mathrm{ISR}$ CR shows that $\epsilon_{\tau\mathrm{ID}}$ is well-understood.
- Contributions of $W/Z$+Jets and $t\bar{t}$ backgrounds to the SR are well-understood (2016/2017).
- The Full Data Driven method seems to be the best strategy to estimate the QCD Multijets contribution in the SR. The shape is extracted from CRB and it will be reweighted using the 2D histogram and the corresponding $p_T(\tau_h)$ weights.
- We exclude $\tilde{\chi}_2^0/\tilde{\chi}_1^{\pm}$ with masses below 290 GeV
- We exceed the current bound of other stau searches

$m(\tilde{\chi}_1^{\pm}) - m(\tilde{\chi}_1^0) = 50$ GeV and $m(\tilde{\tau}) = \frac{1}{2}m(\tilde{\chi}_1^{\pm}) + \frac{1}{2}m(\tilde{\chi}_1^0)$ GeV.

*Thanks*

# BACKUP SLIDES

# Particle Algorithm and $\tau$ properties

## Particle Flow Algorithm

- The algorithm reconstructs the stable visible particle individually in each sub-detector.
- The information recollected by all sub-detectors is combined.
- The visible particles are divided in groups: Photons, electrons, neutral and charge hadrons and muons.
- This information is used to reconstruct high level objects as: The Jets, $E_T^{miss}$ and $\tau$s

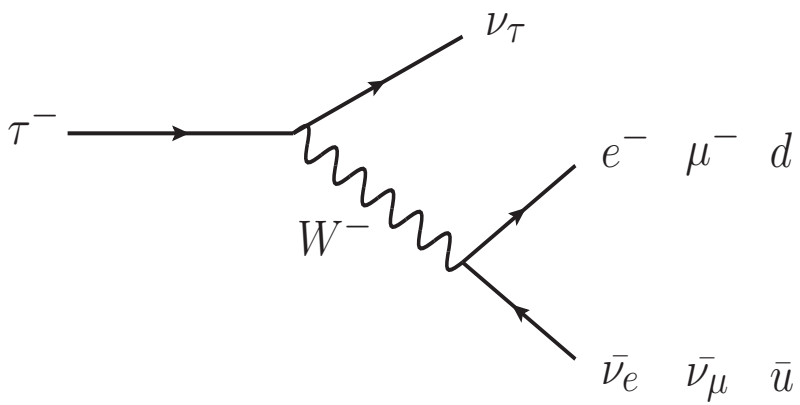


Feynman diagram for $\tau$ decay modes

## General Properties

- $m_\tau = 1.777$ GeV
- $t_{lifetime}(\tau) = 290.6$ fs
- $c\tau = 87\mu m$

### Leptonic Decay

| | |
|---|---|
| $\tau^\pm \rightarrow e^\pm \nu_e \nu_\tau$ | 17.8% |
| $\tau^\pm \rightarrow \mu^\pm \nu_\mu \nu_\tau$ | 17.4% |

### Hadronic Decay

| | |
|---|---|
| $\tau^\pm \rightarrow h^\pm \nu_\tau$ | 11.5% |
| $\tau^\pm \rightarrow h^\pm \pi^0 \nu_\tau$ | 26.0% |
| $\tau^\pm \rightarrow h^\pm \pi^0 \pi^0 \nu_\tau$ | 10.8% |
| $\tau^\pm \rightarrow h^\pm h^\pm h^\mp \nu_\tau$ | 9.8% |
| $\tau^\pm \rightarrow h^\pm h^\pm h^\mp \pi^0 \nu_\tau$ | 4.8% |

- In the leptonic decay the $\tau$ decays too fast, in general, it is no possible to distinguish the $e/\mu$ that come from the other collision. On the other hand, in the hadronic decay the signature is similar to the QCD multijet background. Therefore, an algorithm for $\tau$ identification is needed.

# $\tau$ reconstruction

## Hadron plus strips Algorithm (HPS)

- This Algorithm takes the Jet as a input and reconstruct the individual decay mode, the three decay modes are shown in the following table:

| Decay Mode | |
|---|---|
| 1-prong | $\tau^{\pm} \rightarrow h^{\pm}\nu_{\tau}$ |
| 1-prong+$n\pi^0$ | $\tau^{\pm} \rightarrow h^{\pm}\pi^0\nu_{\tau}$ |
| | $\tau^{\pm} \rightarrow h^{\pm}\pi^0\pi^0\nu_{\tau}$ |
| 3-prong | $\tau^{\pm} \rightarrow h^{\pm}h^{\pm}h^{\mp}\nu_{\tau}$ |

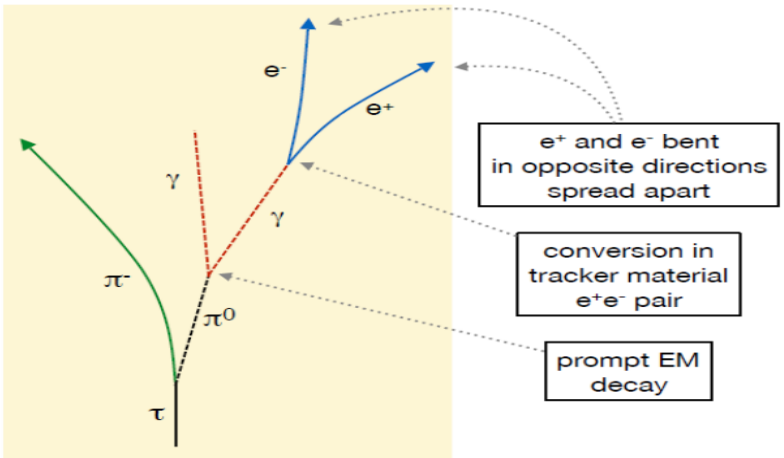


- The $\pi^0$ decays into $\gamma\gamma$, these photons probably can be produce a electron-positron pairs, therefore, these objects are clustered in the ECAL strip in the plane $(\eta, \phi)$
- The $\tau$ candidate is reconstructed using the clustered strip in the ECAL and the charge particles tracks coming from the Jets.

## Possible Fake Candidates:

- QCD jets: Compose by charge ($\approx$ 65 %) and neutral ($\approx$ 20 %) hadrons and photons ($\approx$ 15 %)
- Electrons: Could be misidentified as $h^{\pm}$ or $h^{\pm}\pi^0$ decay modes of the $\tau$.
- Muons: Could be misidentified as $h^{\pm}$ decay mode of the $\tau$.

In order to distinguish the different physics objects, there are discriminants dedicated to tag correctly the $\tau$

# $\tau$ isolation discriminators

## MVA-based Isolation discriminators

- The QCD jets have a larger multiplicity of particles that the $\tau$ jets
- The $\tau$ jets in general, have a narrower cones that the QCD jets.
- Depends on the strong of the selection, there are different working points. For example, the Tight isolation has a identification efficiency of $\approx$ 60% and a fake rate of $4.4 \times 10^{-3}$

## Against electron discriminators

- Base on the amount of Bremsstrahlung associated to the leading track and the multiplicity of particles.
- The Loose isolation has a identification efficiency of $\approx$ 83% and a fake rate of $4.4 \times 10^{-2}$

## Against muon discriminators

- Base on the hits in the muon chambers and low deposits of energy in the ECAL and HCAL.
- The Tight isolation has a identification efficiency of $\approx$ 99% and a fake rate of $1.4 \times 10^{-3}$

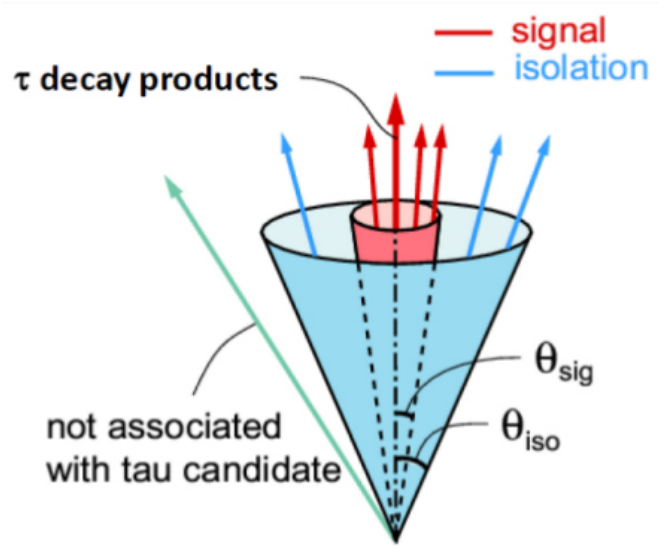

# Background: $\mu \rightarrow \tau_h$ emulation in W+Jets

## Lepton universality:

- For additional confidence in our BG estimates, we follow a second methodology: select muon control sample in data, and then replace muon by $\tau$s using response templates. $p_T^{\tau gen}$ is the $p_T$ before the $\tau$ decays.

  $\sigma(p_T^{\mu}) < 2\% \rightarrow p_T^{\mu} \approx p_T^{\tau gen}$ $\qquad$ $Response = R(p_T^{\tau gen}) = p_T^{\tau_h, RECO} / p_T^{\tau gen}$

- Take $p_T^{\mu}$ in data, we assume it's $\approx p_T^{\tau gen}$, and generate random $p_T^{\tau_h, RECO}$ using the response templates from MC (left side).
- Weights are applied to correct for reconstruction and identification efficiencies.
- Perform closure tests in both MC and data. Data closure test (right side) are performed in a sample orthogonal to the SR, containing small signal contamination, such that, signal-like cuts except require $40 < p_T^{\tau_h, RECO} < 60$ GeV.

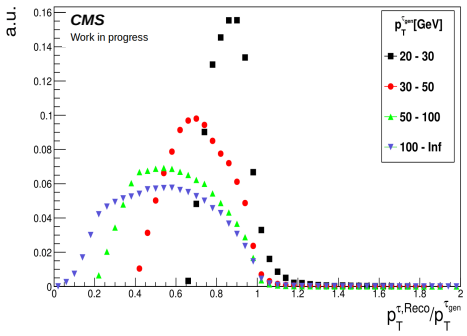


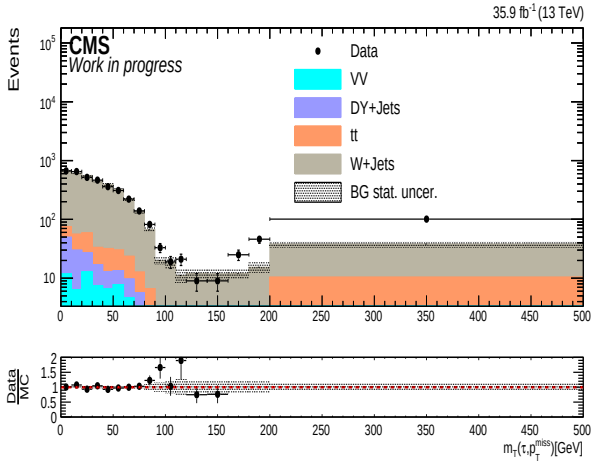


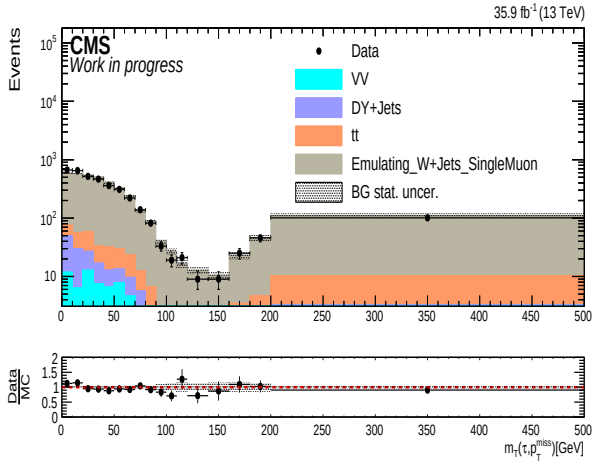

| Source | $W+jets$ | $Z+jets$ | $t\bar{t}$ | $VV$ | QCD-Multijets | Signal |
|---|---|---|---|---|---|---|
| Luminosity | 2.5 | 2.5 | 2.5 | 2.5 | 2.5 | 2.5 |
| ID($\mu$) | $< 1$ | $< 1$ | $< 1$ | $< 1$ | $< 1$ | 1 |
| ID($e$) | $< 1$ | $< 1$ | $< 1$ | $< 1$ | $< 1$ | 1 |
| ID($\tau_h$) | 6 | 8 | 9 | 9 | – | 9 |
| ID($b-jets$) | 2 | 2 | 7 | 2 | 2 | 2 |
| Trigger | 3 | 3 | 3 | 3 | 3 | 3 |
| JES | $s$ | $s$ | $s$ | $s$ | – | $s$ |
| TES | $s$ | $s$ | $s$ | $s$ | – | $s$ |
| MMS | $< 1$ | $< 1$ | $< 1$ | $< 1$ | – | $< 1$ |
| EES | $< 1$ | $< 1$ | $< 1$ | $< 1$ | – | $< 1$ |
| Pileup | 5 | 5 | 5 | 5 | – | 5 |
| Pdf | 4.8 | 4.8 | 4.2 | 3.5 | – | 6.0 |
| bin-by-bin stat | $s$ | $s$ | $s$ | $s$ | – | $s$ |
| Closure+Norm | 2 | 8 | 6 | – | 23 | – |
| $j^{ISR}$ | $s$ | $s$ | – | – | – | $s$ |
| Prefiring | – | – | – | – | – | $s$ |
| Gen. Scale | 1 | 1 | 3.5 | – | – | 2 |
| Fast Sim. | – | – | – | – | – | $s$ |
| $Ratio^{Tight}_{Loose-nonTight}$ | – | – | – | – | $s$ | – |

# Background composition in the SR

- $Z/W/t\bar{t}$/QCD estimations done for 2016 data.

| Central Selections | Yield | Fraction |
|---|---|---|
| VV | $149.9 \pm 7.2$ | 1.2% |
| SingleTop | $202.1 \pm 5.7$ | 1.7% |
| DY | $232.0 \pm 5.0$ | 2.0% |
| tt | $1002.2 \pm 19.3$ | 8.6% |
| QCD | $1359.9 \pm 18.6$ | 11.7% |
| W+Jets | $8596.1 \pm 60.5$ | 74.4% |
| Total Back | $11542 \pm 67.0$ | |
| SignalLSP150 $\times$ 10$X$ | $6398.6 \pm 603.9$ | |

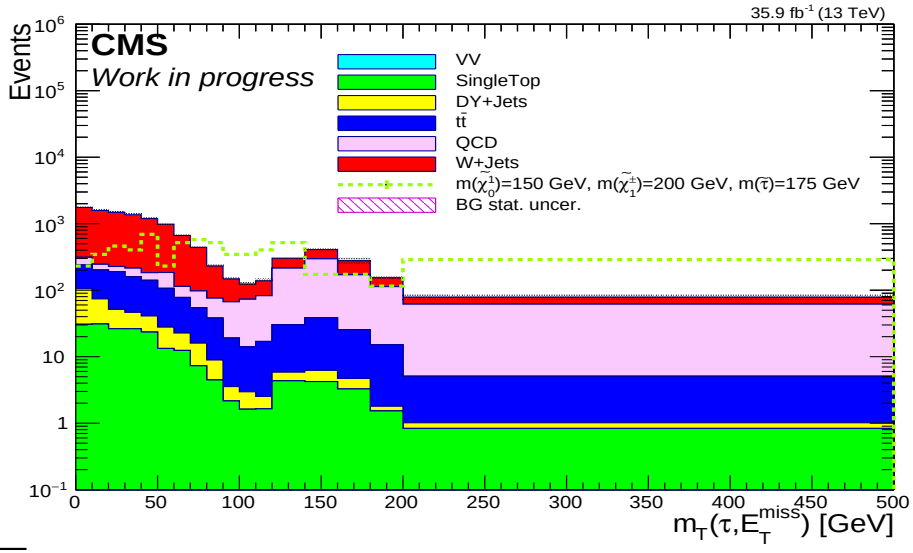

# Sub-detectors

1. Tracker System

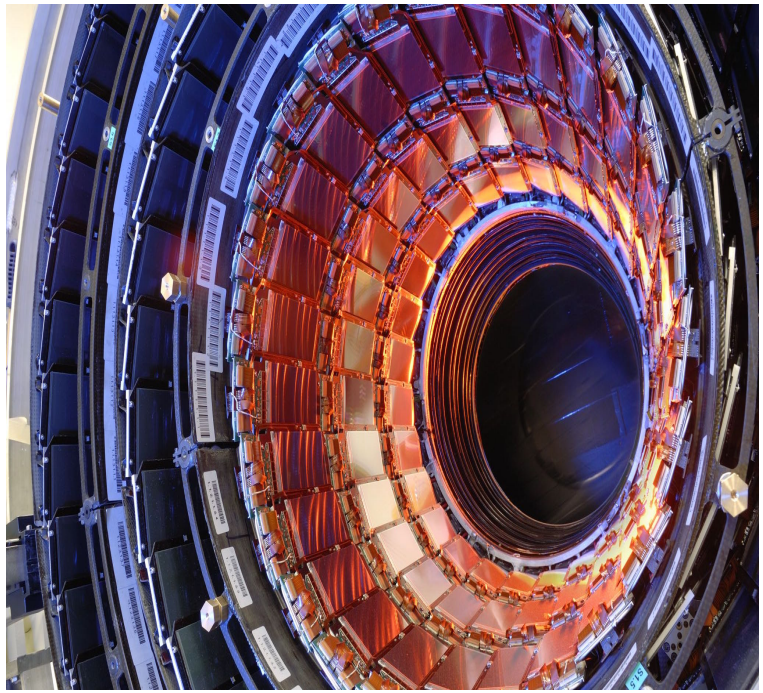

# Sub-detectors

1. Tracker System
2. Electromagnetic Calorimeter ECAL

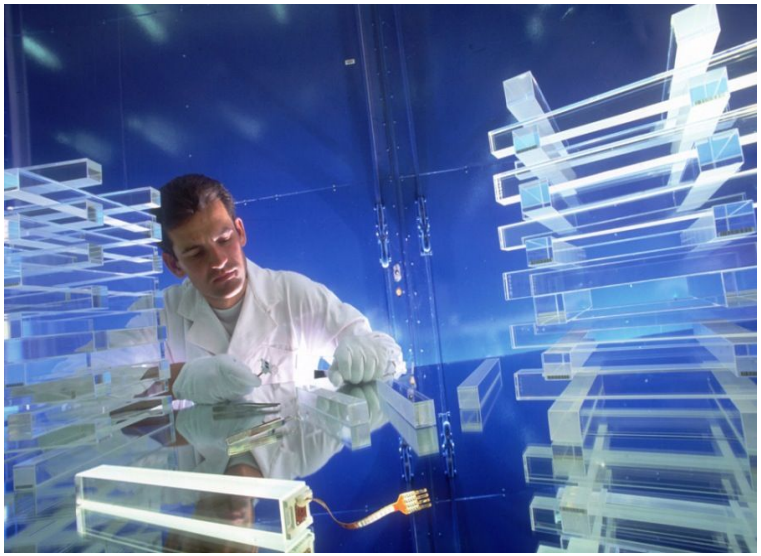

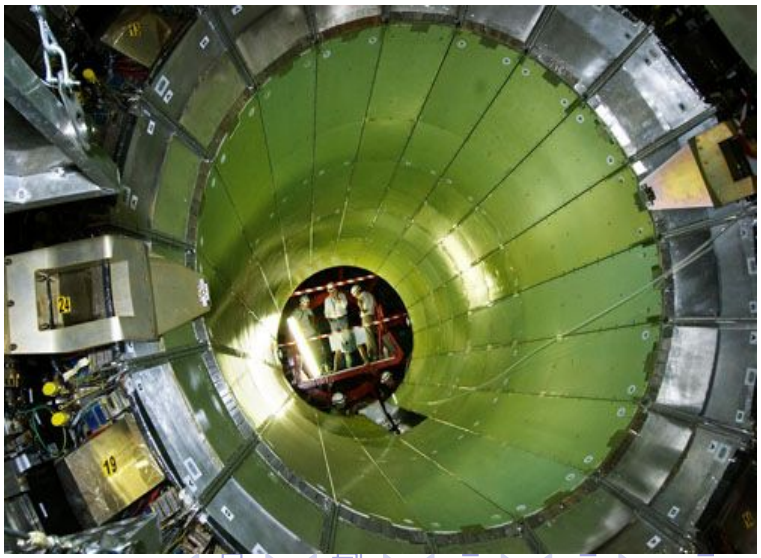

# Sub-detectors

1. Tracker System
2. Electromagnetic Calorimeter ECAL
3. Hadronic Calorimeter HCAL

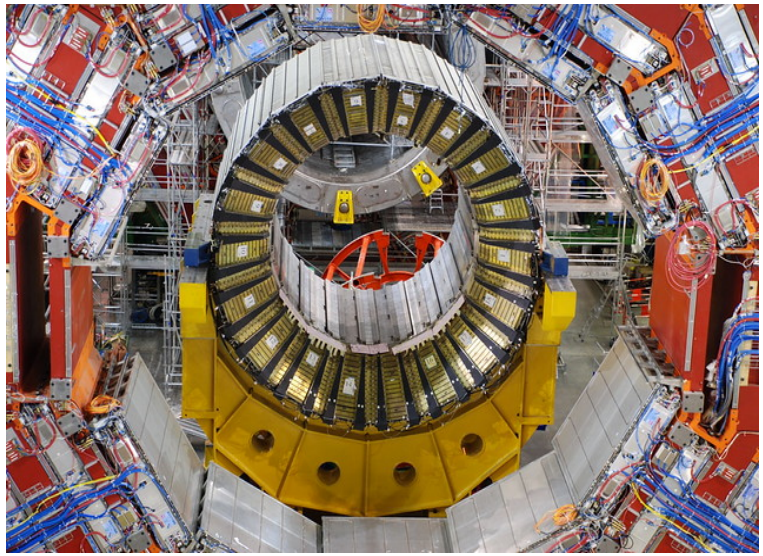

# Sub-detectors

1. Tracker System
2. Electromagnetic Calorimeter ECAL
3. Hadronic Calorimeter HCAL
4. Superconducting Solenoid

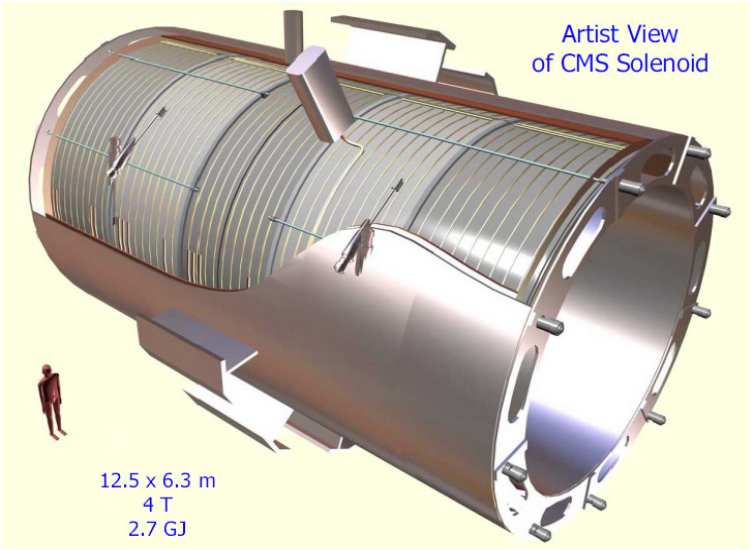


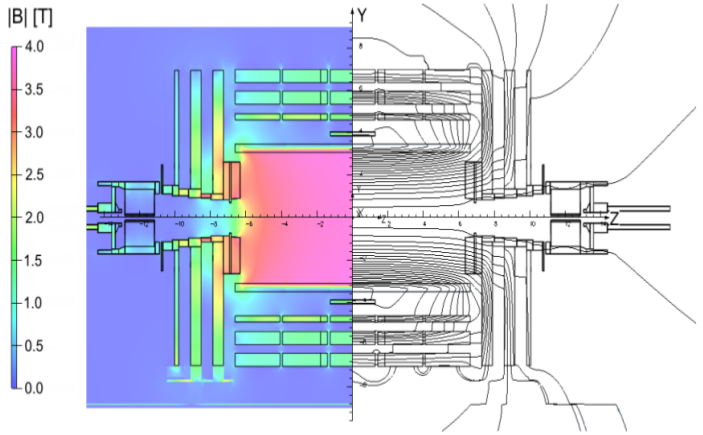


Mapping of the magnetic intensity

# Sub-detectors

1. Tracker System
2. Electromagnetic Calorimeter ECAL
3. Hadronic Calorimeter HCAL
4. Superconducting Solenoid
5. Resistive Plate Chambers (RPC)

Muon system

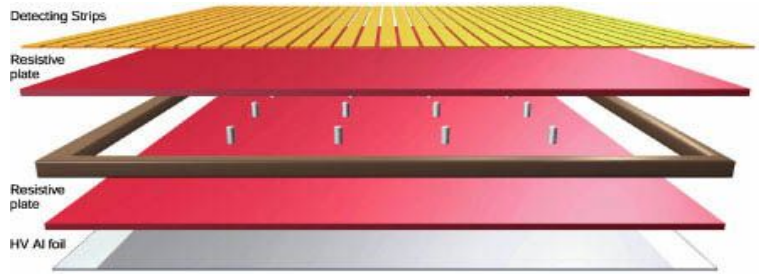

# Sub-detectors

1. Tracker System
2. Electromagnetic Calorimeter ECAL
3. Hadronic Calorimeter HCAL
4. Superconducting Solenoid
5. Resistive Plate Chambers (RPC)
6. Drift Tubes (DT)

Muon system

# Sub-detectors

1. Tracker System
2. Electromagnetic Calorimeter ECAL
3. Hadronic Calorimeter HCAL
4. Superconducting Solenoid
5. Resistive Plate Chambers (RPC)
6. Drift Tubes (DT)
7. Cathode Strips Chambers (CSC)

Muon system

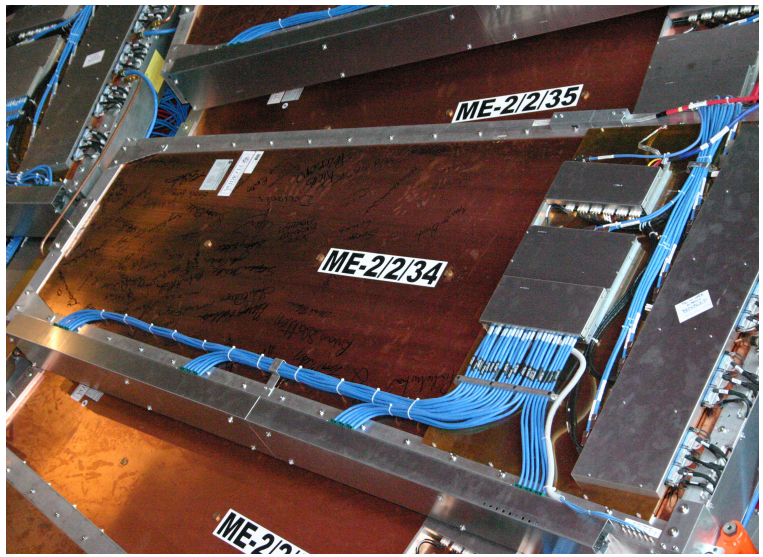

# Sub-detectors

1. Tracker System
2. Electromagnetic Calorimeter ECAL
3. Hadronic Calorimeter HCAL
4. Superconducting Solenoid
5. Resistive Plate Chambers (RPC)
6. Drift Tubes (DT)
7. Cathode Strips Chambers (CSC)
8. $\eta$-partition

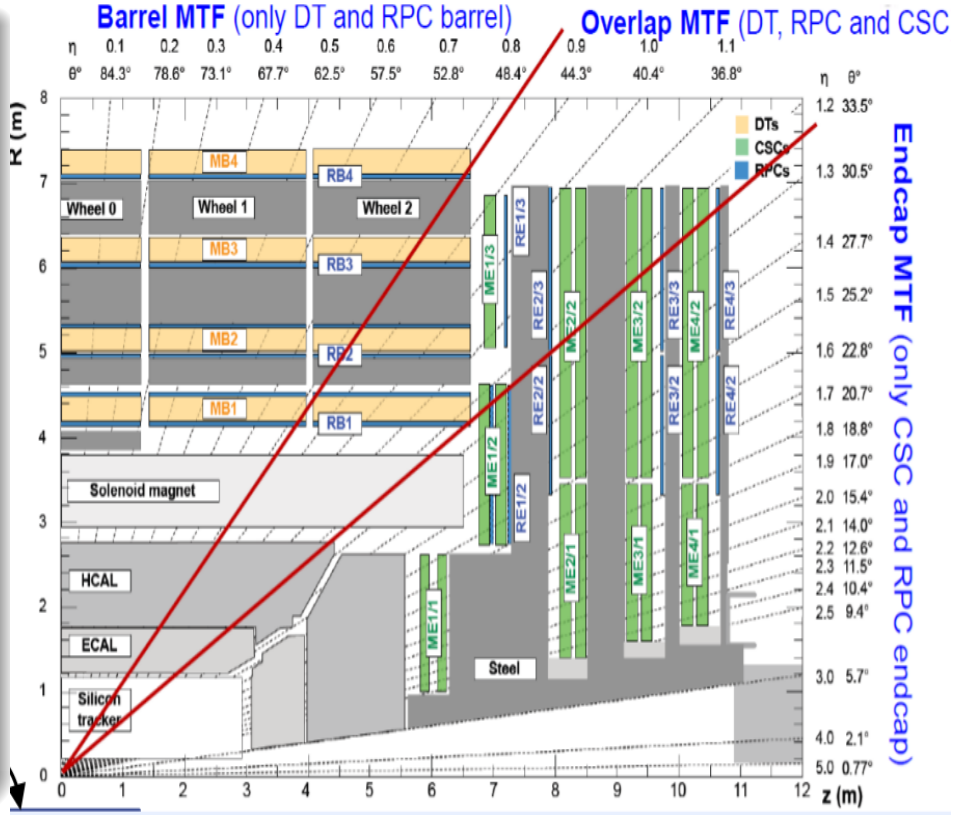

# Trigger esqueme

1. Level 1 Trigger (L1T)

processing of events based on hardware:

- **Too much data to save!**
- **The triggers filter events until a manageable amount of data can be stored!**
  - **40 Million/sec IN**
  - **1000/sec OUT**

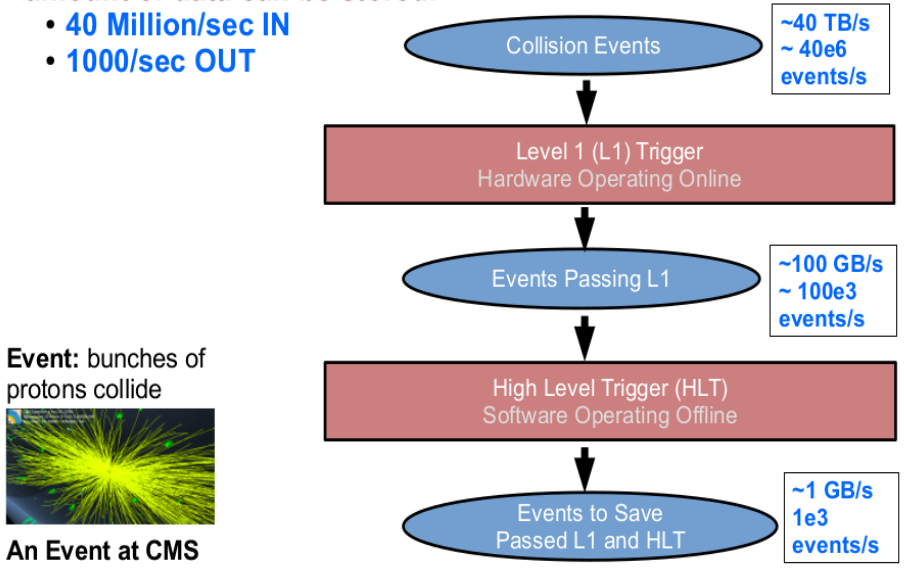


**Event:** bunches of protons collide



**An Event at CMS**

# Trigger esqueme

processing of events based on software:

1. Level 1 Trigger (L1T)
2. High Level Trigger (HLT)

Reconstruction algorithm operate with the information in each read-out to create all physics objects.

# Trigger esqueme

1. Level 1 Trigger (L1T)
2. High Level Trigger (HLT)
3. Data Acquisition System (DAQ)

- The information is saved within a time of 32 $\mu s$.
- The speed is 100 $Gb/s$

# Physics Objects and variables

# Physics Objects and variables

1. Jet
   1. Partonic
   2. Hadronic
   3. Detector

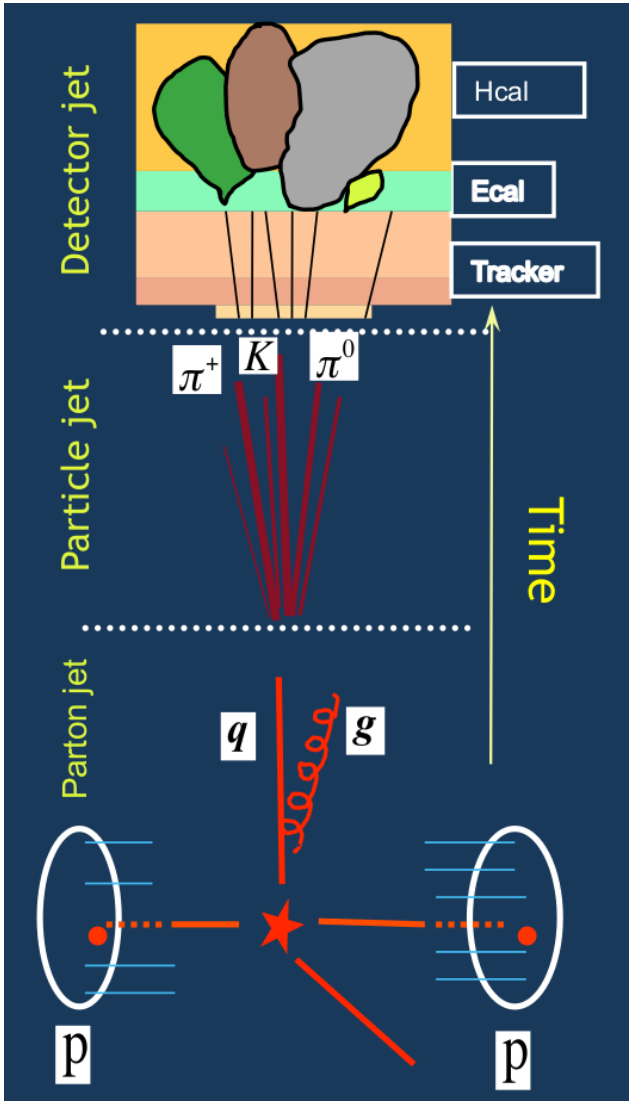

# Physics Objects and variables

1. Jet
   1. Partonic
   2. Hadronic
   3. Detector
2. Jet reconstruction

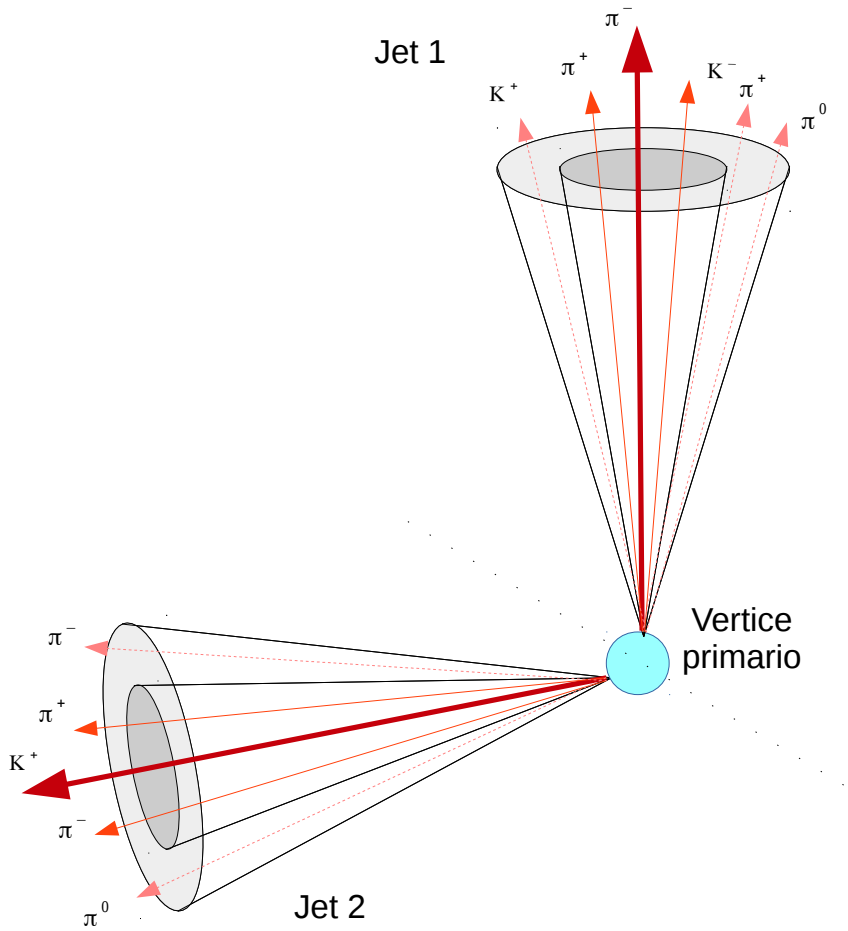

# Physics Objects and variables

1. Jet
   1. Partonic
   2. Hadronic
   3. Detector
2. Jet reconstruction
3. Cross Section

In particle physics, a cross section ($\sigma$) represents the *probability of production* of a specific process. This quantity is related with the level of the interaction between the beam and the target, or between two beams, and it depends on the energy of collisions.

# Physics Objects and variables

1. Jet
   1. Partonic
   2. Hadronic
   3. Detector
2. Jet reconstruction
3. Cross Section
4. Luminosity

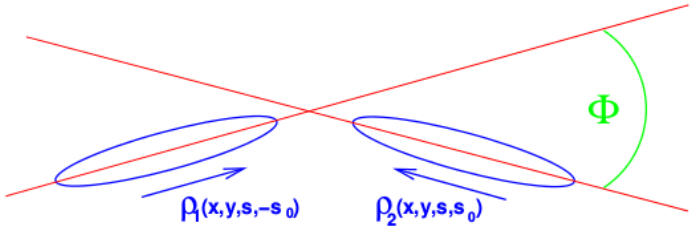


$$\mathcal{L} \sim \frac{N_A \times N_B \times f \times F}{4\pi(\sigma_A \times \sigma_B)} \quad (1)$$

$$L = \int \mathcal{L} dt \quad (2)$$

$$N_i = \sigma_i \times L \quad (3)$$

# Physics Objects and variables

1. Jet
   1. Partonic
   2. Hadronic
   3. Detector
2. Jet reconstruction
3. Cross Section
4. Luminosity
5. Coordinate systems

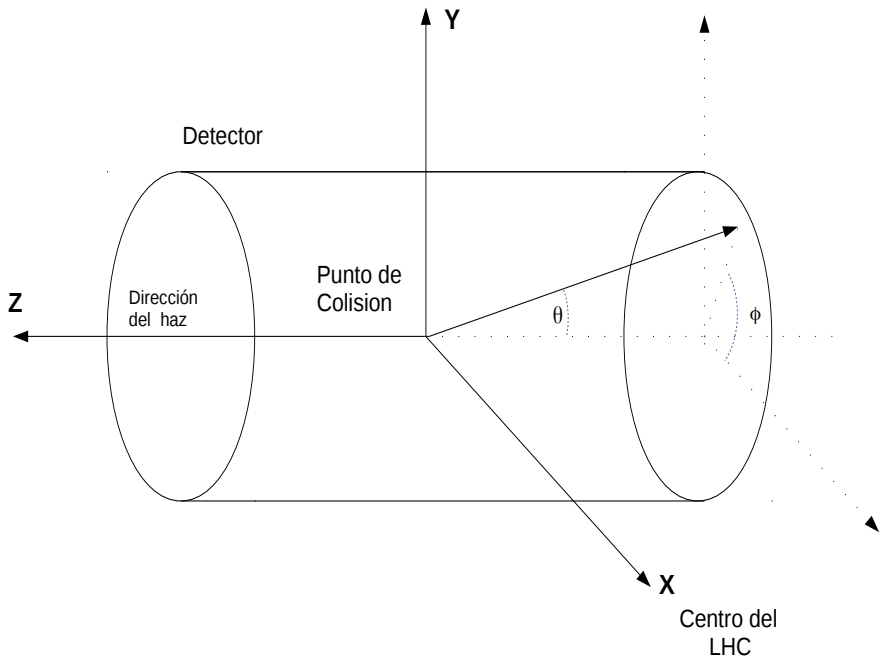

# Physics Objects and variables

$$\eta \equiv -\ln\left[\tan\left(\frac{\theta}{2}\right)\right].$$

1. Jet
   1. Partonic
   2. Hadronic
   3. Detector
2. Jet reconstruction
3. Cross Section
4. Luminosity
5. Coordinate systems
6. Pseudorapidity

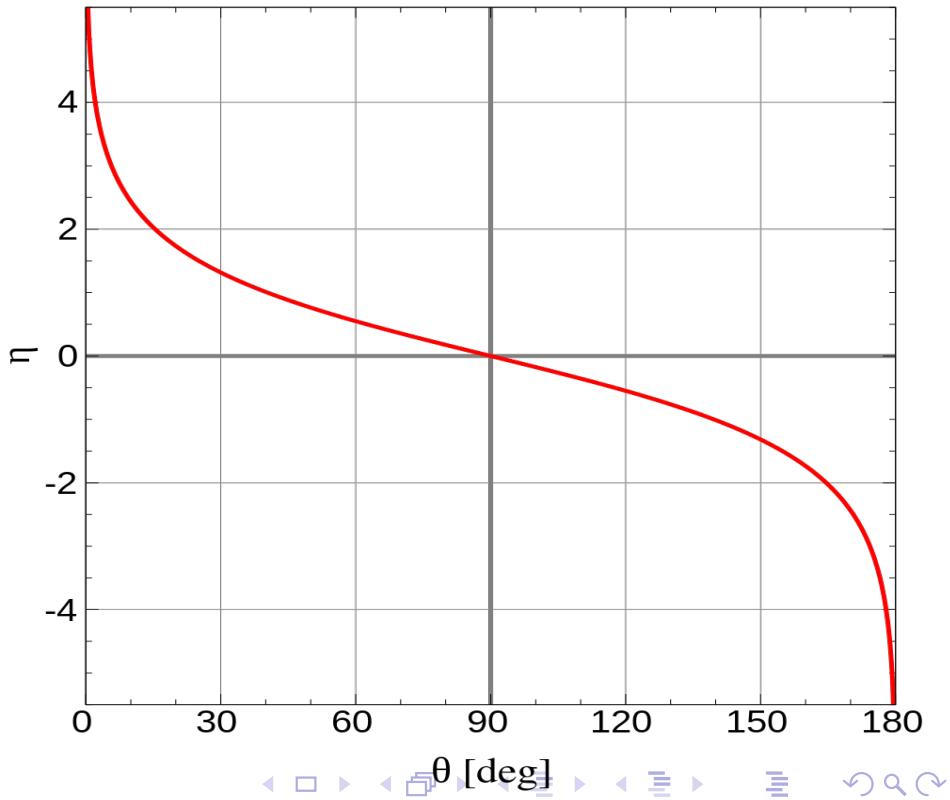

# Physics Objects and variables

1. Jet
   1. Partonic
   2. Hadronic
   3. Detector
2. Jet reconstruction
3. Cross Section
4. Luminosity
5. Coordinate systems
6. Pseudorapidity
7. Missing Transverse Energy $p_{\mathrm{T}}^{miss}$

The momentum conservation in the transverse plane:

$$\sum_i \vec{p}_i^{\,T} = 0,$$

$$= \sum_j \vec{p}_j^{\,T}\,(invisible) + \sum_k \vec{p}_k^{\,T}\,(visible)$$

$$\sum_j \vec{p}_j^{\,T}\,(invisible) = -\sum_k \vec{p}_k^{\,T}\,(visible)$$

$$p_{\mathrm{T}}^{miss} = \Big| -\sum_k \vec{p}_k^{\,T}\,(visible) \Big| \qquad (1)$$